Journal of Physiology (1995), **484.1**, *pp.* 201–225

Synaptic excitation in the thoracic spinal cord from expiratory bulbospinal neurones in the cat

P. A. Kirkwood

Sobell Department of Neurophysiology, Institute of Neurology, Queen Square, London WC1N 3BG, UK

1. Synaptic actions in the thoracic spinal cord of individual expiratory bulbospinal neurones were studied in anaesthetized cats by the use of two techniques: (i) the monosynaptic connections to motoneurones were assessed by cross-correlations between the discharges of the neurones and efferent discharges in the internal intercostal nerves of several segments bilaterally; and (ii) distributions of terminal and focal synaptic potentials were measured by extracellular spike-triggered averaging in the thoracic ventral horn.

2. Monosynaptic connections were identified by both the durations and timings of observed cross-correlation peaks, taking into account accurate conduction velocity measurements derived from collision tests and from spike-triggered averaging. Discrimination was made against peaks resulting from presynaptic synchronization.

3. Monosynaptic connections to motoneurones were identified for twenty-three out of twenty-seven neurones. The connections to nerves on the side ipsilateral to the cell somata were, on average, about 36% of the strength of those on the contralateral side. The overall strength of the connections was about twice as strong as previous estimates for similar connections from inspiratory bulbospinal neurones to phrenic motoneurones. The monosynaptic pathway was calculated to be able to provide most of the depolarization for the motoneurones concerned and therefore was likely to be the main determinant of their firing patterns under the conditions of these experiments.

4. However, taking into account previous measurements it is considered possible that these connections may only involve a minority of motoneurones, perhaps only 10% of the expiratory population. Thus, in general, the control of the whole pool of expiratory motoneurones, despite the strong monosynaptic connections measured here, is suggested to be mainly dependent on spinal interneurones, as has been concluded previously for inspiratory motoneurones.

5. Spike-triggered averaging revealed that nearly all neurones gave signs of collaterals in each of the segments investigated (T7, T8 or T9), as shown by the presence of terminal potentials or focal synaptic potentials, but the projection within a given thoracic segment was non-uniform, in that large-amplitude potentials were more common in the rostral than the caudal part of the segment. This non-uniformity could be a factor involved in the apparently non-heterogeneous connections to the motoneurones.

The majority of long descending pathways to the mammalian spinal cord do not make their principal connections directly on spinal motoneurones, though there are notable exceptions (for reviews see Shapavalov, 1974; Porter & Lemon, 1993). Even in those cases where a monosynaptic connection to motoneurones can be demonstrated, the quantitative functional significance of the connection (i.e. in a given motor act, how much of the drive to the motoneurones concerned is derived from this connection) has usually not been determined.

The respiratory system is just such a case (see Monteau & Hilaire, 1991, for a review). The inspiratory drive from the medulla to the phrenic motoneurones is generally accepted as having a strong monosynaptic component and the intercostal motoneurones with similar inspiratory activity patterns are generally viewed as receiving much less. However, the details of these projections remain as areas of disagreement between different studies and the situation is compounded by the different methods employed, mostly either spike-triggered averaging of

intracellularly recorded EPSPs in motoneurones or cross-correlation between medullary and efferent nerve discharges. These two methods are similar in principle, but they can show quantitative disparities, arising from differences in the parameters assessed or from different sampling biases.

For the expiratory drive to thoracic motoneurones the situation is even less clear. In a small sample of pairs of expiratory bulbospinal neurones and motoneurones, Kirkwood & Sears (1973) demonstrated some (presumed) monosynaptic EPSPs. Cohen, Feldman & Sommer (1985) confirmed this result by cross-correlation, showing histogram peaks consistent with a monosynaptic connection. The peaks were detected frequently, but the particular correlation methods used did not allow the strength of the connection to be assessed. Subsequently, Merrill & Lipski (1987) concluded that the connection was weak: in a relatively large sample of intracellular spike-triggered averages (57 cell pairs), they found only two EPSPs.

The experiments described here were done to re-investigate this issue by using cross-correlation methods, but this time quantified in the same way as has been used already for the better-established inspiratory connection to phrenic motoneurones (Davies, Kirkwood & Sears, 1985*a*, *b*). As in that study, possible errors resulting from synchronization of inputs were taken into account, to be as careful as possible to include only those interactions resulting from a monosynaptic link. This analysis is supported by measurements from extracellular spike-triggered averaging, which confirm the timing relationships which are essential in establishing the direct link. They also give more detailed information on the projection patterns of each bulbospinal neurone within a segment. These patterns not only may have interesting functional and developmental significance in their own right but also are important in the overall functional interpretation of the connections revealed by the cross-correlation analysis.

A preliminary report has appeared (Kirkwood, 1990).

METHODS

Preparation

Measurements were made on thirteen adult cats of either sex anaesthetized with sodium pentobarbitone (initial dose 37·5 mg kg^{-1} I.P., then I.V. as required), paralysed with gallamine triethiodide (subsequent to surgery) and artificially ventilated via a tracheal cannula with oxygen-enriched air, to bring the end-tidal CO_2 fraction initially to about 4%. CO_2 was then added to the gas mixture to raise the end-tidal level to a value sufficient to give a brisk respiratory discharge in the mid-thoracic intercostal nerves (typically 6–7%). Anaesthesia was assessed by continuous observations of the patterns of the respiratory discharges and the arterial blood pressure (measured via a femoral cannula) together with responses, if any, of both of these to a noxious pinch of the forepaw. Only minimal, transient, responses were allowed before supplements (5 mg kg^{-1}) of pentobarbitone were administered. The animal was mounted, prone, by vertebral clamps at about T4 and T10, a clamp on the iliac crest and a plate screwed to the skull. The head was somewhat ventroflexed. Rectal temperature was measured and maintained between 37 and 38 °C by a heating blanket. The bladder was emptied manually at intervals. The animals received occasional infusions of 5% dextran in saline and their systolic blood pressures were above 100 mmHg throughout.

The following nerves were prepared for stimulation or recording via platinum wire electrodes: the internal intercostal nerve; a bundle of dorsal ramus nerves (as in Kirkwood, Munson, Sears & Westgaard, 1988) on the left side of one segment (T7 or T8), in which recordings with a tungsten microelectrode were to be made; and the left external intercostal nerve of T7 or a more rostral segment. Internal intercostal nerves of up to two more segments (T6–T9) on the left and up to two segments on the right were also prepared for recording efferent discharges. In addition, in some animals, the first intramuscular branch of the internal intercostal nerve (a 'filament') was also prepared for recording (Sears, 1964*b*). Discharges in the external intercostal nerve were used to define the timing of central inspiration.

A thoracic laminectomy (caudal T6 to rostral T10) was made, the dura opened and small patches of pia removed from the dorsal columns of T7 or T8. A pressure plate was lightly applied to one of these segments. This plate contained recording wires for assessing, via the cord dorsum volleys, stimulus strengths to the nerves. An array of four insulated stainless steel needles for stimulating either side of the spinal cord was inserted to a depth of about 3·5 mm in T9 or T10 segments as in Kirkwood *et al.* (1988). The laminectomy and nerves on both sides were submerged in a single paraffin oil pool constructed from skin flaps. An occipital craniotomy was made, the dura opened and a small patch of pia removed from the right side of the medulla 0–3 mm caudal to obex. The general arrangement of electrodes is shown in Fig. 1*A* (dorsal ramus nerves omitted).

Recording

A glass-insulated, platinum-black-coated tungsten microelectrode (Merrill & Ainsworth, 1972), with 25–50 μm of tip exposed, was inserted into the left side of the spinal cord via a hole in the pressure plate, using an angle of 15 deg to the vertical in the transverse plane. Positions were determined for the maximum amplitudes of the motoneurone antidromic field potentials resulting from stimuli to the internal intercostal and the dorsal ramus nerves at five times nerve threshold. The site of the maximum amplitude dorsal ramus field potential was used as a reference position for subsequent recordings, as in Kirkwood *et al.* (1988). The tungsten electrode was then left ready at a suitable position in the ventral horn for recording spike-triggered averages of field potentials (see below).

A glass microelectrode (external tip diameter ~3 μm, filled with 3 M NaCl) was introduced into the medulla, via a hole in a small pressure plate, to record unit activity in the right caudal nucleus retroambigualis. The activity of single units was recorded extracellularly via a conventional bandpass amplifier. Expiratory bulbospinal neurones with axons descending as far as T9 or T10 were identified by antidromic responses to stimuli (0·1 ms pulses) delivered via the electrodes on one or other side of the cord at T9 or T10. Identification was always confirmed by a collision test and by double stimuli to show that the minimum interval in the collision test was not due to soma refractoriness.

Procedures and analysis

A period of 13–71 min from each single unit recording, together with nerve recordings and a tracheal pressure signal to show the phasing of the respiratory pump (52 cycles min^{-1}), were recorded on magnetic tape. Subsequently (and sometimes on-line) the times of occurrence of spikes in the medulla and nerves were acquired for cross-correlation analysis and analysed for connections between the bulbospinal neurone and motoneurones as described by Davies *et al.* (1985*a*). The only difference between then and now was in the selection of spikes from the nerve recordings by the window discriminators. For the filaments used in Davies *et al.* (1985*a*, *b*), the criteria for separating α- and γ-discharges are fairly clear (Sears, 1964*b*). For the whole-nerve recordings here, the signal-to-noise ratio was lower (cf. Fig. 1) and the criteria are less clear. Window levels were usually set to accept spikes greater than 30–50% maximum amplitude, or so that there was always a brief gap in the accepted spikes between the end of inspiration and the start of the expiratory burst. These two criteria gave similar levels for the examples in Fig. 1, the gap being about 0·4 s in duration. This setting was chosen to exclude spikes from units with continuous (tonic) discharges such as are typical of γ-motoneurones (Sears, 1964*b*). For brisk discharges such as those in Fig. 1 there is little doubt that most of the accepted spikes were from α-motoneurones (for nerves of this

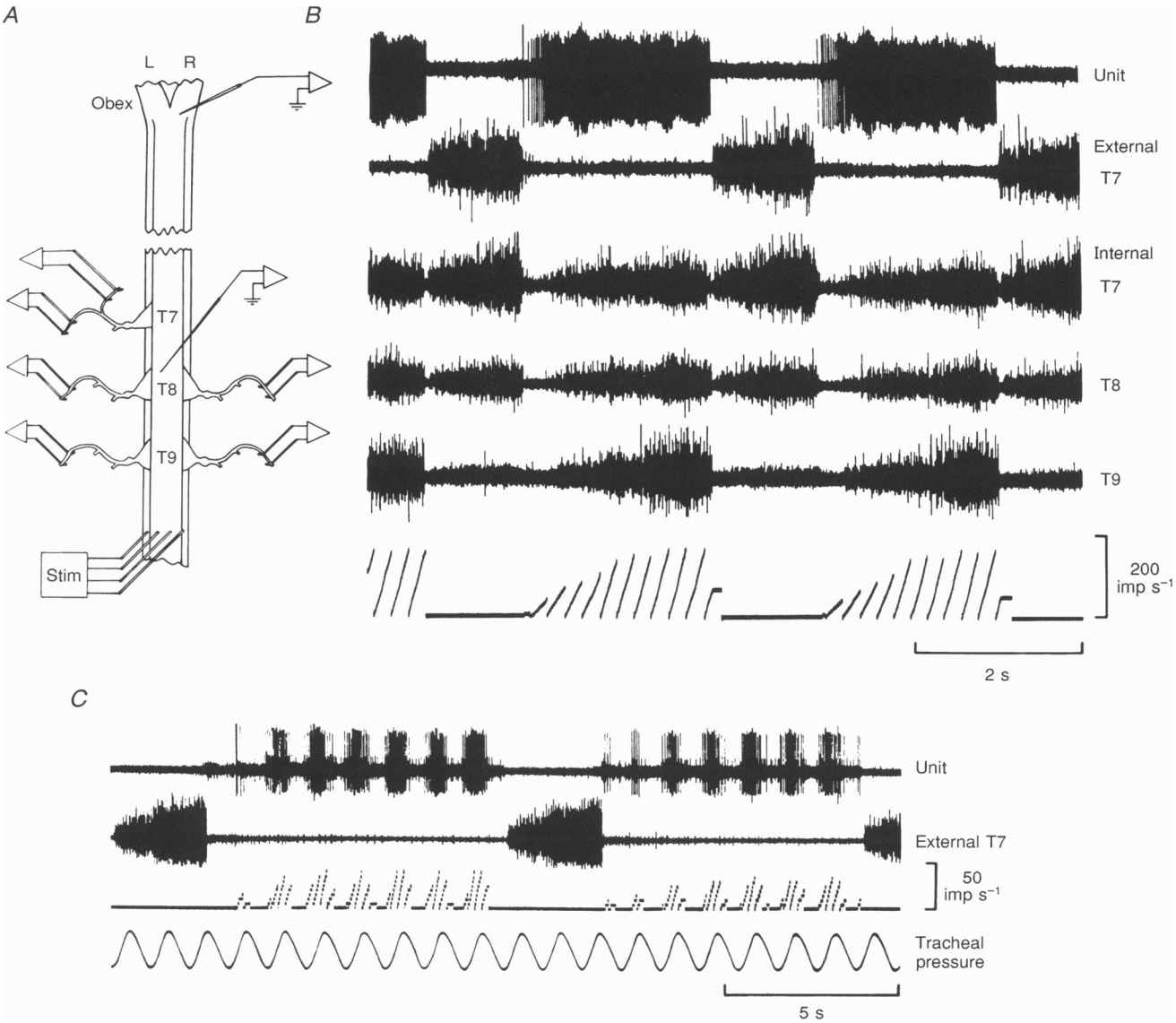

Figure 1. Recording methods and raw data

A, general recording arrangements (see text). The number of nerves used varied but the most common arrangement is shown. A single external intercostal nerve recording is shown at T7 in addition to the internal nerves used in the other segments. Stim, stimulating electrodes. *B*, a sample of the data from magnetic tape, nerves as indicated. Lowest trace, rate-meter output for the unit recording. Note the reverse gradients of activity, inspiratory activity highest in T7, expiratory in T9. *C*, an example of a recording from a unit with a strongly pump-modulated firing pattern. Tracheal pressure signal (uncalibrated) shows the timing of the ventilator (positive up).

thickness γ-spikes would, in any case, be expected to be near the noise level), but when the discharges were less frequent it is possible that γ-spikes were included. The accepted spikes included large numbers that were inspiratory as well as those that were expiratory, particularly in the more rostral segments (cf. Fig. 1*B*). However, the inspiratory spikes did not feature in the correlation analysis since they occurred in the opposite phase of respiration to the bulbospinal discharges. Firing patterns for the bulbospinal neurones were assessed off-line from a rate-meter record (Fig. 1*B* and *C*). Peaks in correlation histograms were accepted as significant if a single bin exceeded $3{\cdot}29\sqrt{m}$ (Sears & Stagg, 1976), where m was the baseline count, as in Davies *et al.* (1985*a*). Single bin counts exceeding this limit (which will sometimes occur by chance) were ignored if they fell outside the range of expected latencies (0–10 ms; Davies *et al.* 1985*a*).

The projections of units to the left thoracic ventral horn were also assessed by spike-triggered averaging of the signal (bandpass filtered, usually 3 dB at 10 Hz and 10 kHz) from the tungsten electrode. Tracking was performed with the tungsten electrode as described in Results, usually using 4096 sweeps at each site. Sometimes the averages were done in two halves of 2048 sweeps each to assess reproducibility. The rostrocaudal position of the electrode was determined with respect to the rostral end of the segment, defined by the most rostral dorsal root entry point. Usually there is a 1–2 mm gap between the most caudal dorsal root bundle of one segment and the most rostral bundle of the segment below. Occasionally a very fine filament leaves the rostral bundle and enters the cord with the caudal bundle of the segment above. Such fine rootlets were ignored in defining the segmental boundaries. Postmortem, the distances from obex to the recording site(s) and to the T9 or T10 stimulating electrodes were measured *in situ* by exposing the whole length of cord and laying a thread along it.

In a few instances the tungsten electrode was used for microstimulation instead of, or as well as, for recording. In these instances a non-plated electrode, pulses of 0·1 ms in duration and currents of up to 100 μA, measured via a 100 Ω resistor in the reference line, were used. Averaged potentials in the illustrations that follow are shown with the convention positive up.

RESULTS

General properties of the bulbospinal neurones and their axons

Thirty-four expiratory bulbospinal neurones were studied, located 0–4 mm caudal to obex, thirty of them identified by antidromic activation from T9 or T10 (29 contralaterally, 1 ipsilaterally) and confirmed by collision. The other four were identified by recording spike-triggered averages of axonal potentials from T7 contralaterally. One of these four failed to give an antidromic spike when tested with the T9 or T10 stimulus, two gave an apparent antidromic spike, but collision was uncertain for one and difficult to test (a combination of a fast firing rate and long conduction time) for the other, and the fourth was not tested.

Firing patterns were assessed for twenty-eight units which were used for cross-correlation analysis or spike-triggered averaging. Approximate modal firing rates, estimated from the first peak or shoulder in the autocorrelation histogram of the unit, ranged from 33 to 200 impulses s^{-1} (mean ± S.D., 107 ± 49 impulses s^{-1}). The firing rates of all units showed an incrementing pattern during expiration. However, for some animals (5 out of 13, 12 units) respiration was slow (cycle duration > 10 s) and, with the prolonged expiratory phases involved, units could show a plateau of firing rate after an initial ramp of duration 1–3 s. Only eight units started to fire immediately after the end of inspiration (within 0·4 s). The remainder started to fire 0·8 s or more into expiration, presumably in stage II (Richter & Ballantyne, 1983). Although cycle-triggered histograms were not constructed, it was clear from inspection of firing rate plots that none of the units would have been of the step-ramp pattern if classified as in Cohen *et al.* (1985). Twenty-four units were definitely of the ramp type (e.g. Fig. 1*B*) and one unit showed a small initial step. The remaining three were of a type which would not have been seen by Cohen *et al.* (1985) with their cycle-triggered pump, namely those in which the discharges showed 100% modulation by the respiratory pump in addition to the restriction of firing in expiration (Fig. 1*C*). The ramp units also often showed some pump modulation, modulation being strong (> 50%) for three units.

Microstimulation was used in T8 to identify the axonal position for four units and the presence of collaterals for two of these. Figure 2*A* shows examples of threshold *vs.* depth plots used in these determinations, the electrode tracks being illustrated in Fig. 2*B*. The threshold minimum at depth 4·1–4·2 mm on track B is indicative of an axon in the white matter, whereas the narrower trough more dorsally on track A, within the ventral horn, is indicative of a collateral with a lower conduction velocity (Davies & Kubin, 1986). Latencies of activation (2·15 ms ventrally, 2·5 ms dorsally) confirmed this, as did the two spike-triggered average recordings (Fig. 2*C*), which showed a typical axonal waveform ventrally but at the dorsal focus a terminal potential (TP) at a longer latency, followed by a focal synaptic potential (FSP; Munson & Sypert, 1979; Dick, Viana & Berger, 1988).

The positions of two other axons in the lateral funiculus were determined by spike-triggered averaging alone (Dick & Berger, 1985; Fig. 2*D*). The positions of all six axons are shown in Fig. 2*B* and are scattered widely in the lateral–ventrolateral funiculi, confirming the observations of Merrill (1971) in more rostral segments.

In the majority of experiments spike-triggered averaging was used alone, without microstimulation. Tracking was restricted to the ventral horn and the precise position of the stem axon was not determined. However, for several axons an attenuated version of the axonal spike appeared in the average as a 'remote' axonal potential, such as in Fig. 2*D*, particularly in the more ventral recordings at both rostrocaudal levels, as indicated at 2·15 ms rostrally (*a–f*)

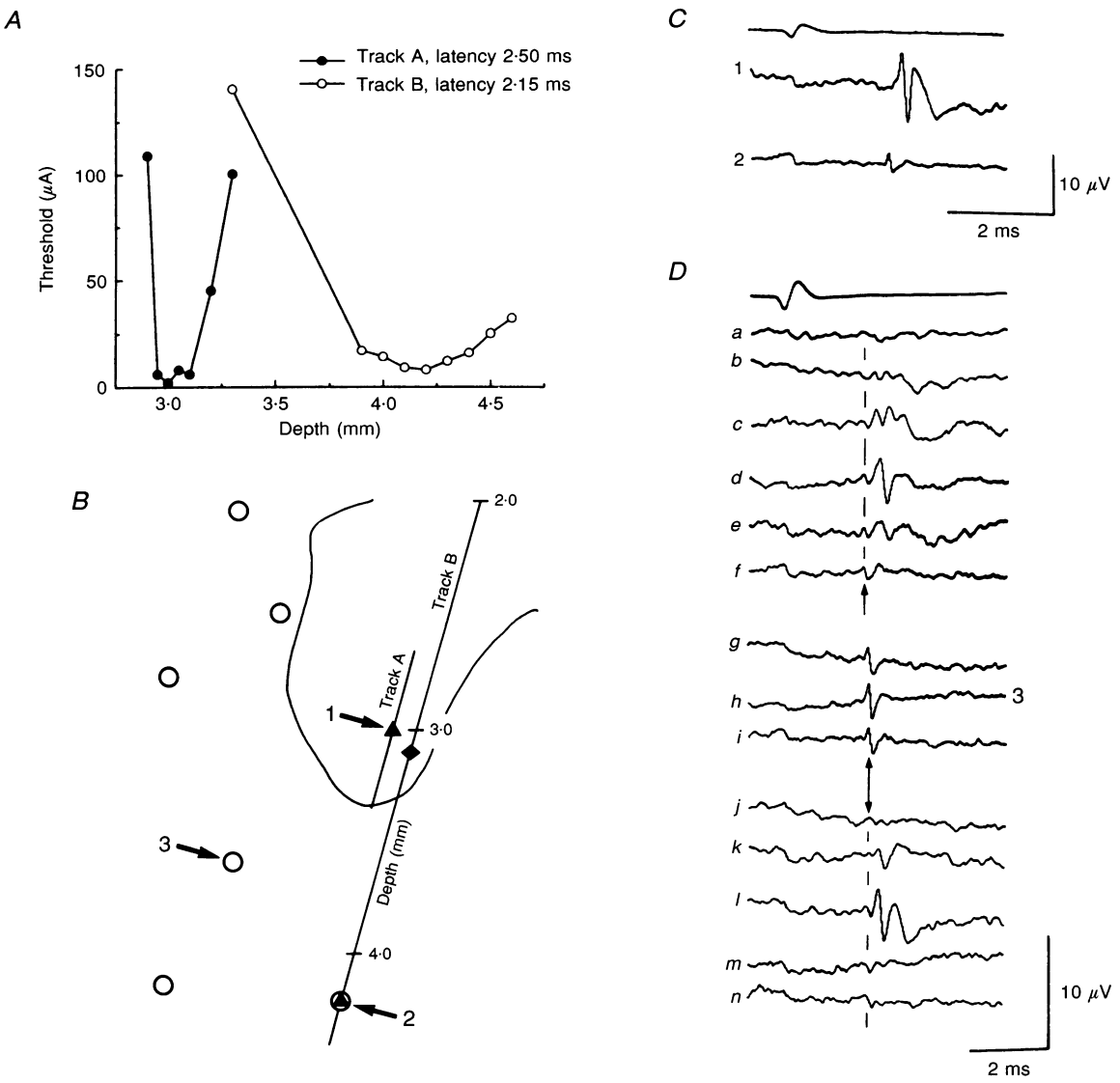

Figure 2. Determination of stem axon positions and timing of axon spikes

A, depth–threshold plots for a single bulbospinal axon with microstimulation. Plots are shown for two electrode tracks 0·1 mm apart, as shown in *B*. The narrow minimum for the plot of track A and long latency of the response indicate a slowly conducting collateral at 3·0–3·1 mm deep. The broad minimum and short latency for track B indicate a fast-conducting axon at a depth of 4·2 mm (▲, sites 1 and 2, respectively in *B*). *B*, axon positions for six units (circles) estimated either as in *A* or by spike-triggered averaging. Positions calculated from microdrive co-ordinates with reference to the position of the maximum-amplitude antidromic field potential for the dorsal ramus (Kirkwood *et al.* 1988; ◆). Outline of ventral horn represents an average as in Kirkwood *et al.* (1988). *C*, spike-triggered averages of potentials from sites 1 and 2 for the unit involved in *A* and *B*. Note the clear TP and FSP at site 1 and the slightly earlier, small axon potential at site 2. *D*, spike-triggered averaging on three tracks for a different unit. *a–f*, a track through the ventral horn at a rostral location in the segment, with sites 0·25 mm apart, at depths 1·85 (*a*) to 3·1 mm (*f*; reference depth 2·7 mm). *g–i*, three sites at depths 2·85, 3·1 and 3·35 mm, respectively on a track 0·6 mm lateral to the reference point (depth 2·6 mm) and 6·6 mm caudal to *a–f*. *j–n*, five sites 0·25 mm apart, at depths 2·1 (*j*) to 3·1 mm (*n*) on a track 0·5 mm medial of *g–i*. Single-headed arrow indicates the time of the deflections corresponding to the axon spikes rostrally (latency 2·15 ms) and the double-headed arrow, the same caudally (latency 2·30 ms). These deflections are each largest at the ventral sites for *a–f* and *j–n*, corresponding to the position of the axon, taken as that for *h*, indicated as 3 in *B*. Sites in the ventral horn show TPs and FSPs. Note (rare) complex TP in *c*. Top traces in *C* and *D* are the averaged trigger spike.

and 2·30 ms more caudally (*j–n*; also see Fig. 9*B*). The variation in amplitude of these early potentials (for some units largest in a dorsolateral position, for others ventrally) confirmed the widespread distribution of axonal positions.

Conduction velocities of bulbospinal axons

Conduction times for individual units were needed to establish the timings of the axonal spike in different segments, and conduction velocities were needed because their distribution was used to establish a criterion for assessing presynaptic synchronization effects in the cross-correlation histograms (Davies *et al.* 1985*a*).

Conduction times were calculated from the critical interval in the collision test, performed at 2 × axon threshold. The critical interval (50% response) was measured to the nearest 0·05 ms as the time from approximately 20% amplitude on the rising phase of the negative unit spike to the start of the stimulus pulse. Conduction time was defined as 0·5 ms (assumed axonal refractory period) less than this. This is the same procedure as in Davies *et al.* (1985*a*) which was then justified *a priori*, but which now can be justified empirically. In Fig. 3*A* the conduction times to T7 or T8 (●), calculated from the conduction times to T9 or T10 via the collision test as above, are compared with the observed conduction times for axonal spikes obtained by spike-triggered averaging as described in the preceding section, these times being measured to the baseline crossing at the start of the negative phase of the axonal spike. The agreement is close for a wide range of conduction times, all points being within 0·18 ms of the line of identity. In the interpretation of peaks in cross-correlation histograms this collision test method was used consistently to give the times of arrival of axonal spikes in each segment, except for the four units mentioned above where the collision test was not available or not considered reliable. For these four, the spike-triggered average measurements were used.

In an attempt to check whether the deviations from equality that remained for the conduction times estimated by collision test (Fig. 3*A*, ●) were due to variations in axonal refractory period, the method of Swadlow (1982) was also used. This employs a double stimulus within the critical period of the collision test to give a direct assessment of the refractory period, which can then be used with the collision test in place of the assumed value of 0·5 ms. Fourteen out of twenty refractory periods in this test were between 0·45 and 0·65 ms but the remainder ranged from 0·25 to 0·9 ms. For seven units direct comparisons were made between conduction times calculated this way with the values from spike-triggered averaging (Fig. 3*A*, ○). The deviations from equality were no less by this method than for those calculated from the collision test method. In particular two of three extreme values (refractory periods 0·8 and 0·25 ms, data points indicated on the graph) gave larger deviations than when a refractory period of 0·5 ms was assumed. Thus, in our hands, the Swadlow test gives no improvement over the simple assumption of 0·5 ms for axonal refractory period.

The distribution of conduction velocities for the bulbospinal units is shown in Fig. 3*B*, together with the

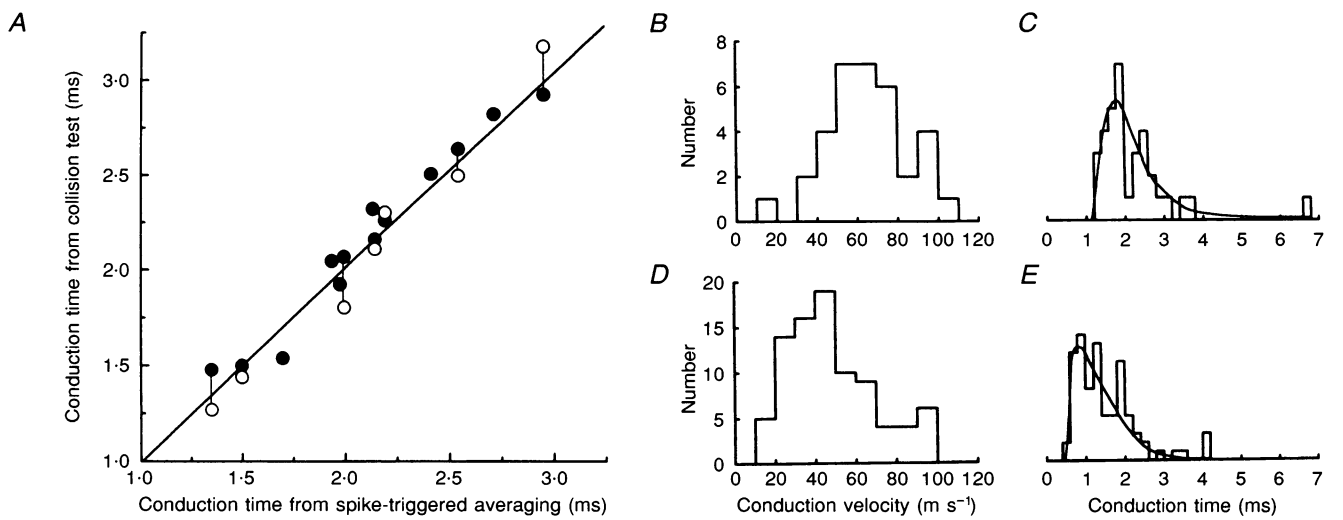

Figure 3. Conduction time and conduction velocity measurements

A, validation of collision test estimation of conduction time by comparison with that measured by spike-triggered averaging. Each filled point corresponds to one unit. Open points show values calculated using the method of Swadlow (1982) to estimate the refractory period at the stimulation site in place of an assumed 0·5 ms. Vertical lines join these to the corresponding points using the assumed 0·5 ms. The line of equality is also shown. *B*, distribution of conduction velocities measured here. *C*, corresponding distribution of conduction times to rostral T7. The smooth curve was fitted by eye. *D* and *E*, as *B* and *C*, but for the data of Davies *et al.* (1985*a*; conduction times to the level of the phrenic motor nucleus).

Table 1. Sampling statistics of unit–nerve pairs

		Numbers of units tested					Numbers of histograms with peaks					
		No. of nerves					Narrow		Medium width			
		1	2	3	Total		s.	n.s.	s.	n.s.	None	Total
						Contralateral						
A	$m \geqslant 1082$	7	5	7	19	B	24	3	5	4	2	38
	$m \geqslant 121$	4	9	14	27		35	6	6	10	7	64
						Ipsilateral						
C	$m \geqslant 1082$	1	9	—	10	D	6	2	1	1	9	19
	$m \geqslant 121$	3	15	—	18		9	2	1	3	18	33

A and C, numbers of units tested with the indicated numbers of nerves (one nerve for each segment) contralateral or ipsilateral to the unit recording, as indicated. B and D, numbers of histograms observed with the indicated types of peaks (one histogram calculated for each unit–nerve pair, m being the baseline count for each histogram). s., significant peaks; n.s., not significant (see text).

comparable distribution for inspiratory neurones from Davies *et al.* (1985*a*; Fig. 3*D*). Despite covering a very similar range, the expiratory neurones clearly have generally faster conducting axons (mean ± S.D. 65·3 ± 18·8 impulses s^{-1}) than the inspiratory neurones (48·4 ± 21·8 impulses s^{-1}) and a less skewed distribution.

The distribution of conduction times to rostral T7 for the bulbospinal units here is shown as a histogram in Fig. 3*C*. Following the logic of Davies *et al.* (1985*a*), the width of the peak in this histogram at half-amplitude (half-width) was taken as the minimum half-width for peaks in the cross-correlation histograms which were likely to arise via presynaptic synchronization. A peak with a half-width less than this was taken as evidence for a monosynaptic connection. The half-width in question was estimated as 1·1 ms, that of the smooth curve (fitted by eye) in Fig. 3*C*. Note that 1·1 ms is coincidentally the same limit as was used by Davis *et al.* (1985*a*, *b*). The criterion there was defined from the slower conduction velocities of Fig. 3*D*, giving much greater temporal dispersion, but for the much shorter conduction distance to the level of the phrenic motor nucleus, as shown in Fig. 3*E*. The mean conduction time here is much less than in Fig. 3*C*, but the half-width of the histogram happens to be about the same.

Cross-correlation analyses

General features of the histograms

Twenty-seven units with contralateral axons were studied in thirteen cats, their discharges being correlated with the efferent discharges in the main internal intercostal nerve trunk of up to three segments contralaterally. Seventeen of these units were also studied in the same way with one or two segments ipsilaterally. Additionally, one unit with an ipsilateral axon was studied with one segment ipsilaterally.

The sampling was inevitably uneven, being dependent on the activity levels in each nerve (cf. Fig. 1). As in Davies *et al.* (1985*b*), only unit–nerve pairs where histograms had a baseline count per bin of at least 121 were accepted as having been tested. This number of counts, via the Poisson-derived confidence limit of Sears & Stagg (1976), allows a peak of amplitude, $k = 1{\cdot}3$, to be detected (i.e. one where the largest bin count is at least 1·3 times the baseline bin counts). (In fact only one of the accepted histograms had less than 271 counts per bin, which allows a peak of $k = 1{\cdot}2$ to be detected.) In addition, separate statistics were kept on those pairs in which weaker effects could be detected, i.e. histograms with mean bin counts of at least 1082, which allows peaks with $k = 1{\cdot}1$ to be detected. Table 1A and C shows the numbers of units tested for each of these two ranges for different numbers of segments.

Most histograms showed peaks of some kind (Table 1B and D). Examples of types of peaks are shown in Fig. 4, which includes peaks with half-widths $< 1{\cdot}1$ ms, and Fig. 5, where the half-widths are mostly $> 1{\cdot}1$ ms. Generally these two types were categorized as 'narrow' resulting from a monosynaptic connection, and 'medium width', probably resulting from presynaptic synchronization, as in Davies *et al.* (1985*a*). Sometimes these two types were present together. Figures 4 and 5 include examples of separations of the two types and illustrate some of their properties. These properties could be more clearly observed than in Davies *et al.* (1985*a*) because high frequency oscillations (HFO), which are a common component of inspiratory discharges, were not present in the expiratory discharges.

Figure 4*A* shows a typical narrow peak in isolation. No broader component is visible and only a very weak periodicity is visible (generally higher counts around a lag of −5 ms than around zero). A periodicity might be expected because of periodic firing of the bulbospinal unit, but in this case the primary peak is relatively weak ($k = 1{\cdot}148$) and the unit was firing with a relatively

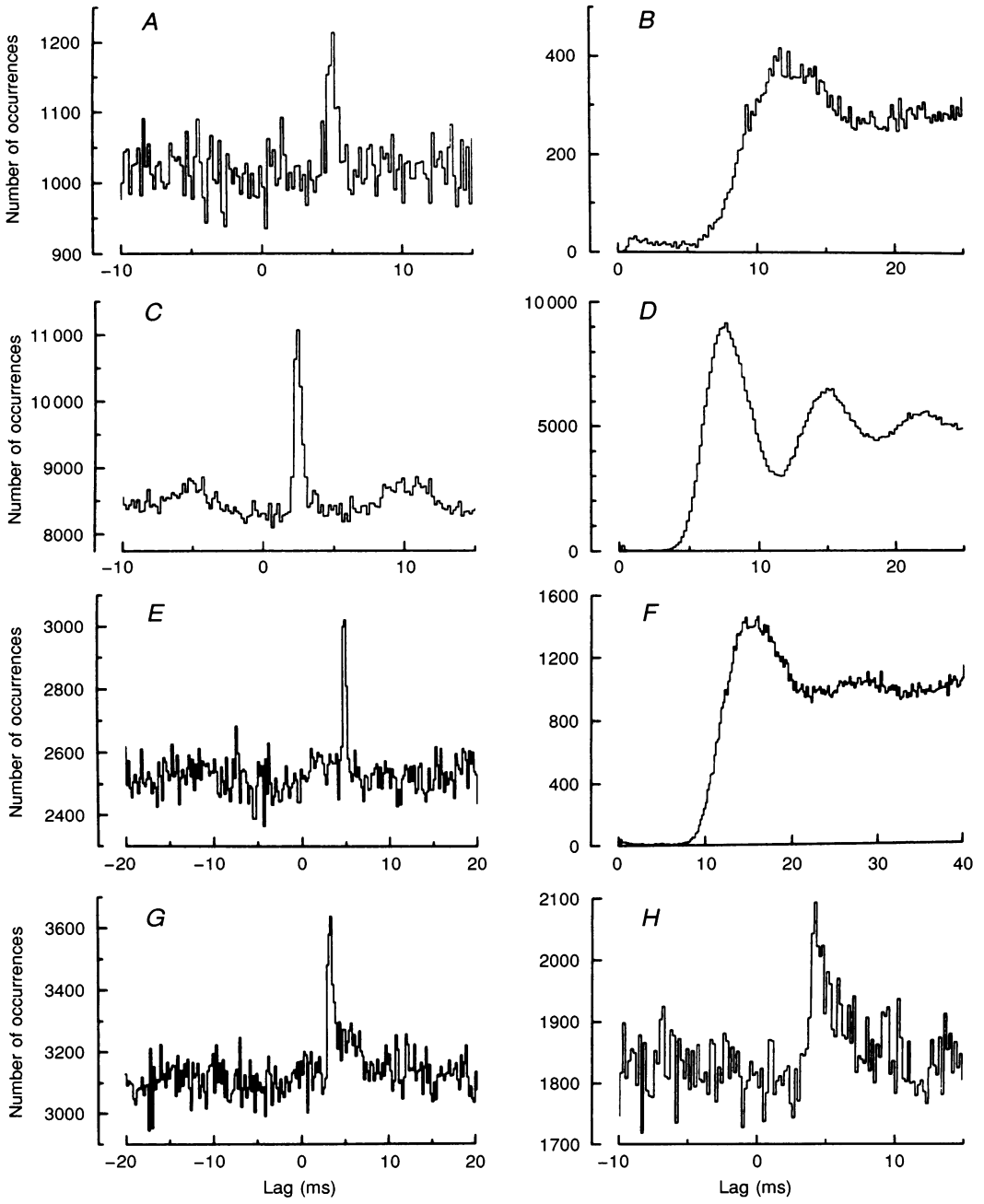

Figure 4. Examples of cross-correlation histograms

Each histogram was constructed from the discharges of a single bulbospinal unit (reference spikes) and the efferent discharges of one internal intercostal nerve. *A*, a typical narrow peak. *B*, autocorrelation histogram for the reference unit of *A*. *C*, an example of a rather stronger narrow peak, where the more periodic firing of the reference unit (autocorrelation histogram shown in *D*) created a periodicity in the cross-correlation histogram (peaks at −5 and +10 ms in *C*). *E*, example of a cross-correlation histogram with a narrow peak accompanied by a weak asymmetric trough (visible to the left of the peak, but not to the right), apparently corresponding to the initial trough in the autocorrelation histogram (*F*). *G*, a cross-correlation histogram showing a similar feature associated with a rather broad weak peak, in addition to a narrow peak (autocorrelation histogram not shown). The conduction velocity of the reference unit in *G* was faster than in *E*. *H*, an example of a narrow peak apparently superimposed on a broader base but without clear points of inflexion that could separate these features. Overall half-width, 1·1 ms. All nerve recordings, except in *H*, were from contralateral segments; the recording in *H* was from an ipsilateral segment: *A*, T9; *C*, T7; *E*, T8; *G*, T7; *H*, T8. Bin widths, 0·192 ms throughout. Note more compressed time scale for *E*–*G*.

variable rate (autocorrelation histogram shown in Fig. 4*B*), so that any secondary peak would, in any case, be weak and broad (centred on 12 ms either side of the primary peak). By contrast Fig. 4*C* shows an example with a stronger primary peak ($k = 1{\cdot}301$), and from a unit firing regularly at a fast rate. For this unit the periodicity of 8·5 ms in the autocorrelation histogram (Fig. 4*D*) also appears as a clear symmetrical feature in the cross-correlation histogram (Fig. 4*C*).

For some units a weak broader component may have been present in addition to a narrow peak (but the overall half-width was still < 1·1 ms), as shown in Fig. 4*E*, *G* and *H*. In *E* the broader component appears as an apparently separate earlier peak, or at least the narrow peak seems to be superimposed on its falling phase. The relatively long latency of the narrow peak is appropriate to the conduction velocity of the unit, which was relatively slow (49·7 m s^{-1}). The unit was not firing at a very constant rate, though a relatively weak peak did appear in its autocorrelation histogram, at 15 ms (Fig. 4*F*). This peak (or at least its preceding trough) seems to be reflected in an asymmetric weak trough to the left of the main peak in the cross-correlation histogram of Fig. 4*E*. A mapping of the periodicity of the reference event only to the left, with no other periodicity being introduced, is evidence for non-periodic common excitation of the unit in the medulla and the motoneurones (i.e. presynaptic synchronization; Moore, Segundo, Perkel & Levitan, 1970). This evidence is additional to the early latency of the broader component, which is alone strong evidence for presynaptic synchronization being the origin of this component.

A somewhat similar combination is seen in Fig. 4*G*, except that here the conduction velocity of the unit was greater (78·5 m s^{-1}) and the narrow peak appears to be situated on the rising phase of a broader component rather than on the falling one. The early foot is not so clear. Also the firing rate of the unit was even less constant than for the example in *E* and *F* (autocorrelation not shown) and so even less of an asymmetrical trough is present. Thus for this example (*G*) on its own there is little direct evidence for the origin of the relatively delayed medium-width component in the peak, which could therefore be interpreted as arising in at least three ways (not mutually exclusive), namely oligosynaptic connections, delayed monosynaptic connections via slowly conducting collaterals, or presynaptic synchronization. However, in both of these two examples the narrow and medium-width components were clearly separable.

In the third example (Fig. 4*H*) a broadish base is present in the peak but no obvious inflexion. As in Fig. 4*G*, interpretation of the broader base could be threefold. No periodicities were present and the auto-correlation histogram was also rather non-periodic. The overall half-width of the peak here is 1·1 ms. Because there was no basis for separating two components, this peak was classified simply as the widest example of the narrow peaks.

Narrow peaks were present for most histograms from recordings with nerves contralateral to the units (24 out of 38 or 35 out of 64, depending on the sampling level chosen; Table 1B), as they were for a reasonable fraction of histograms from ipsilateral nerves (6/19 or 9/33, Table 1D). These peaks were all significant (see Methods) whether the baseline was taken as a point on an underlying medium-width peak (as in Fig. 4*E* and *H*) or as estimated from longer negative or positive lags.

In addition, for eight histograms (6 contralateral nerves, 2 ipsilateral) narrow peaks were apparent by eye but were not quite significant. However, these histograms were not counted as flat and are listed separately in Table 1 because the peaks were all significant when bins were combined to give a wider bin width and the peaks were all at an appropriate latency for a monosynaptic connection when compared with the population as a whole (see later), or when compared with similar significant peaks from the same units in histograms calculated from data obtained in adjacent segments. An example is shown in Fig. 5*A*, *C* and *E*.

Histograms with peaks having half-widths > 1·1 ms fell into two groups. For the first group (7 histograms) the peaks were all significant and all showed a relatively sharp profile that might be supposed to contain a narrow component. However, reliable separation into narrow and medium-width components was not possible for these peaks. Examples are included in Fig. 5. The first of these (*G*) comes from the same unit as Fig. 4*G* and has the same general form, a sharp peak (at monosynaptic latency) superimposed on a weak broader feature. However, the peak is generally weaker and therefore noisier. There appear to be seven bins in the sharp part of the peak and the half-width of the peak was measured as 1·4 ms. Thus, despite its general appearance, the peak had to be classified as medium width rather than narrow.

Figure 5*B* shows a peak with a better signal-to-noise ratio, again with a possibility of a considerable narrow component. There is a weak early foot (latency taken as 2·9 ms) but no reliable inflexion for separating two components. The half-width was 1·2 ms. This histogram is therefore almost the same as Fig. 4*H* but just on the other side of the 1·1 ms half-width criterion. In Fig. 5*D*, however, there is a more prominent early 'foot' (latency taken as 2·7 ms) and the half-width was estimated as 1·9 ms. There is no doubt about classifying the peak as medium width. If a narrow component is present it is again not separable.

In contrast, Fig. 5*F* and *H* shows two examples of histograms in which it was thought safe to classify the

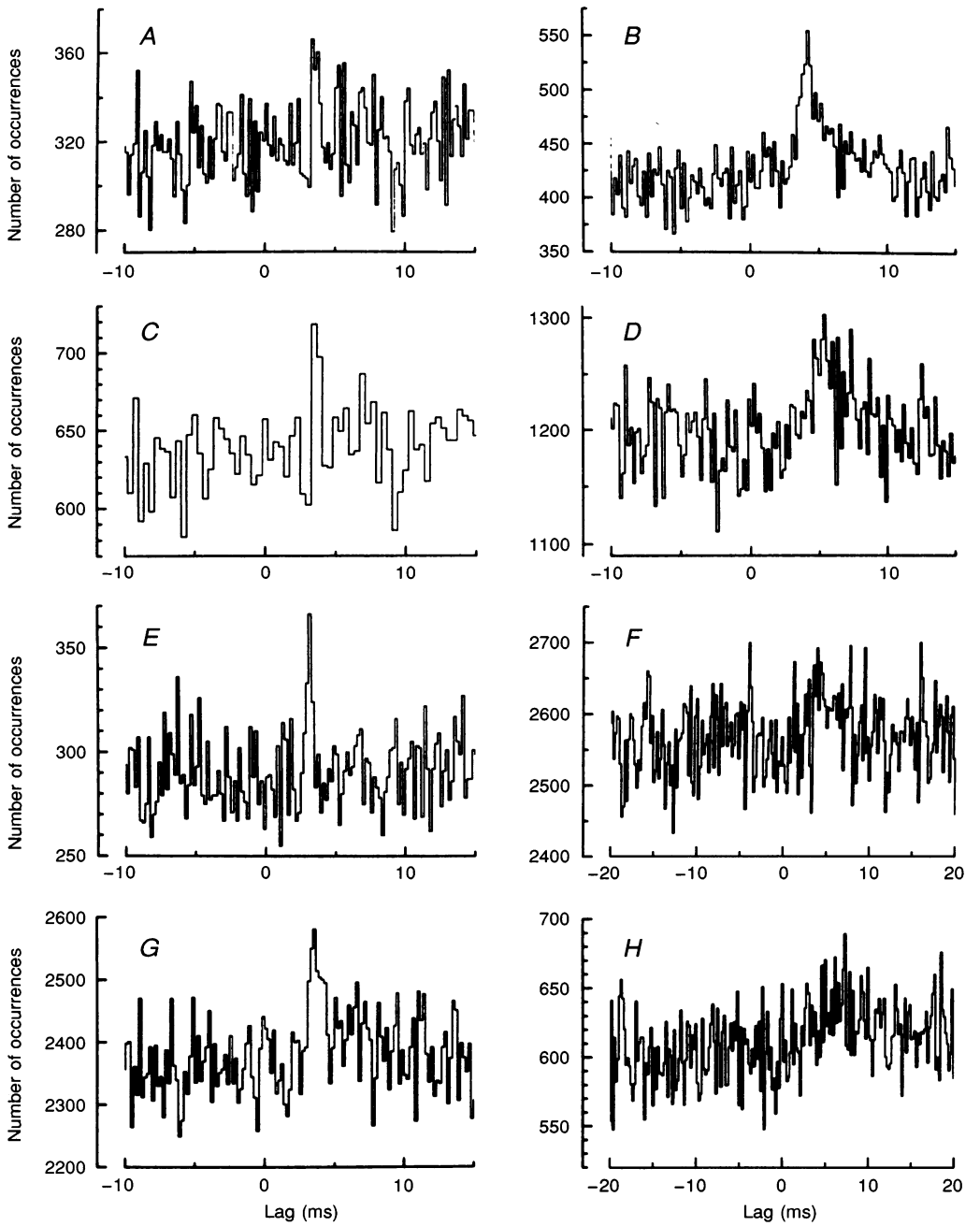

Figure 5. Further examples of cross-correlation histograms

A and *C*, a marginally significant narrow peak, i.e. one which was just not significant with a bin width of 0·192 ms (*A*), but was significant when bins were combined to give a bin width of 0·384 ms (*C*). The peak here (segment T7) is at a similar latency to the peak seen for the same recording epoch for segment T8 (*E*). *B*, histogram which is likely to include a narrow component but has no clear inflexions to separate this from a broader base, so with a half-width of 1·2 ms, it was classified as medium width. *D*, significant peak, unequivocally classified as medium width. *F* and *H*, two examples of non-significant medium-width peaks (*H*, same unit as *D*). *G*, a peak with an apparent narrow component, but a half-width of 1·4 ms and therefore classified as medium width (same unit as Fig. 4*G*). All nerve recordings, except in *B*, were from whole nerves in contralateral segments; the recording in *B* is from a contralateral filament. *A* and *C*, T8; *B*, T9; *D*, T8; *E*, T7; *F*, T9; *G*, T8; *H*, T7. All bin widths except *C*, 0·192 ms. Note more compressed time scale for *F* and *H*.

peaks as only medium width (half-widths here are 1·9 and 9·0 ms). None of the histograms in this group were significant (10 from contralateral nerves, 3 from ipsilateral; Table 1), but because of their durations (half-widths from 1·2 to 9·0 ms) they were all clear by eye and were significant when bins were combined into wider bin widths. The histogram in *H* clearly does not show a narrow peak. It is just possible that a narrow component is present in *F* (as in *B* or *D*), but since the overall peak amplitude is not significant, it follows that no narrow component could be.

In addition to the above, in four cats the discharges of eleven units were correlated with the expiratory discharges in one to three contralateral nerve filaments as well as (or in one instance in place of) discharges in the main nerve trunk. In fourteen histograms with baseline counts above 121, one significant narrow peak, one non-significant narrow peak, three significant medium-width peaks and one non-significant medium-width peak were observed. The proportion of significant peaks is lower than for the discharges in the main nerves, but the averaged baseline count was also lower, being above 1082 for only two histograms.

Distributions of half-widths of peaks from correlations with discharges in contralateral and in ipsilateral nerves are shown in Fig. 6. These two distributions are virtually indistinguishable.

In total only three out of twenty-eight units gave no significant peaks (4/27 if only narrow peaks counted). One of these had an ipsilateral axon tested with only one (ipsilateral) nerve. The other two (tested with one or two contralateral nerves and two ipsilateral ones) came from the group of three units which showed 100% modulation of firing rate with the ventilation pump (Fig. 1*C*). One of these two did give a non-significant narrow peak. One further unit (with a contralateral axon) gave no significant peaks for three contralateral nerves but did give significant peaks for two ipsilateral nerves.

Latencies of peaks

The timings of peaks were considered separately for narrow and medium-width peaks. The latencies of the narrow peaks, measured from the rising negative phase of the trigger spike to the start of the first bin that was judged by eye to have increased counts, were plotted against axonal conduction velocity and showed an obvious relationship (Fig. 7*A*), whereas the latencies of the medium-width peaks plotted in the same way did not (Fig. 7*B*).

More precise timing comparisons came from measurements of transmission delay, which is the latency of the peaks measured from the calculated axonal spike time in individual segments (Davies *et al.* 1985*a*) and thus takes into account conduction distances for individual cats.

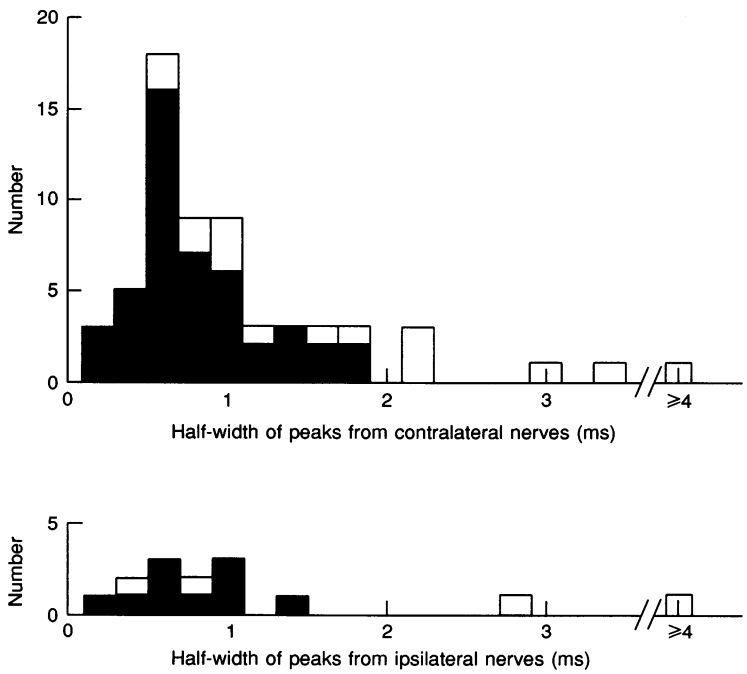

Figure 6. Distributions of half-widths of cross-correlation peaks

Peaks for nerves either contralateral or ipsilateral to the bulbospinal unit somata shown separately, as indicated. ■, significant peaks; □, not significant. Narrow peaks were defined as those with half-widths below 1·1 ms.

Histograms of transmission delays are shown in Fig. 7*C* and *D*. There was little difference between the distributions of delays for the different contralateral segments T7, T8 or T9, mean delays for the narrow peaks being 1·17, 1·29 and 1·26 ms, respectively, not including the delays for non-significant peaks. These, however, seemed to be part of the same distribution (□). The delays for narrow peaks from ipsilateral segments mostly fitted within the same range (fourth histogram in Fig. 7*C*). The two outlying values for significant peaks between 3 and 4 ms both came from a unit with a particularly low axonal conduction velocity (19·2 m s^{-1}; next lowest 38·1 m s^{-1}) and it is not unreasonable that the collaterals of this unit re-crossing to the ipsilateral side of the cord should be significantly slower than those of the other axons.

In contrast, the majority of the medium-width peaks had apparent transmission delays less than those of the narrow peaks, 50% of both the significant or non-significant groups actually being negative. The three significant peaks with negative delays had half-widths of 1·2, 1·4 and 1·9 ms. Because of their short delays, these peaks, or at least the early parts of them (e.g. Fig. 5*D*) could only have arisen via presynaptic synchronization, which further justifies the value of 1·1 ms as the dividing line between the two main types of peak.

Amplitudes of peaks

Distributions of k (see Methods) for the different categories of peaks are shown in Fig. 8. The values for the narrow peaks were calculated in three cases after the separation of low-amplitude, medium-width peaks (e.g. Fig. 4*E* and *H*). For both contralateral and ipsilateral nerves the narrow peaks had larger amplitudes than the medium-width peaks. In assessing the strengths of the monosynaptic connection only the narrow peaks are strictly relevant. For contralateral nerves the mean value of k was 1·16 for either sampling level ($n = 35$ or $n = 24$). When the non-significant peaks were included the mean became either 1·15 or 1·14 for the two levels, respectively ($n = 41$ or $n = 27$). When the flat histograms and non-significant medium-width peaks were included

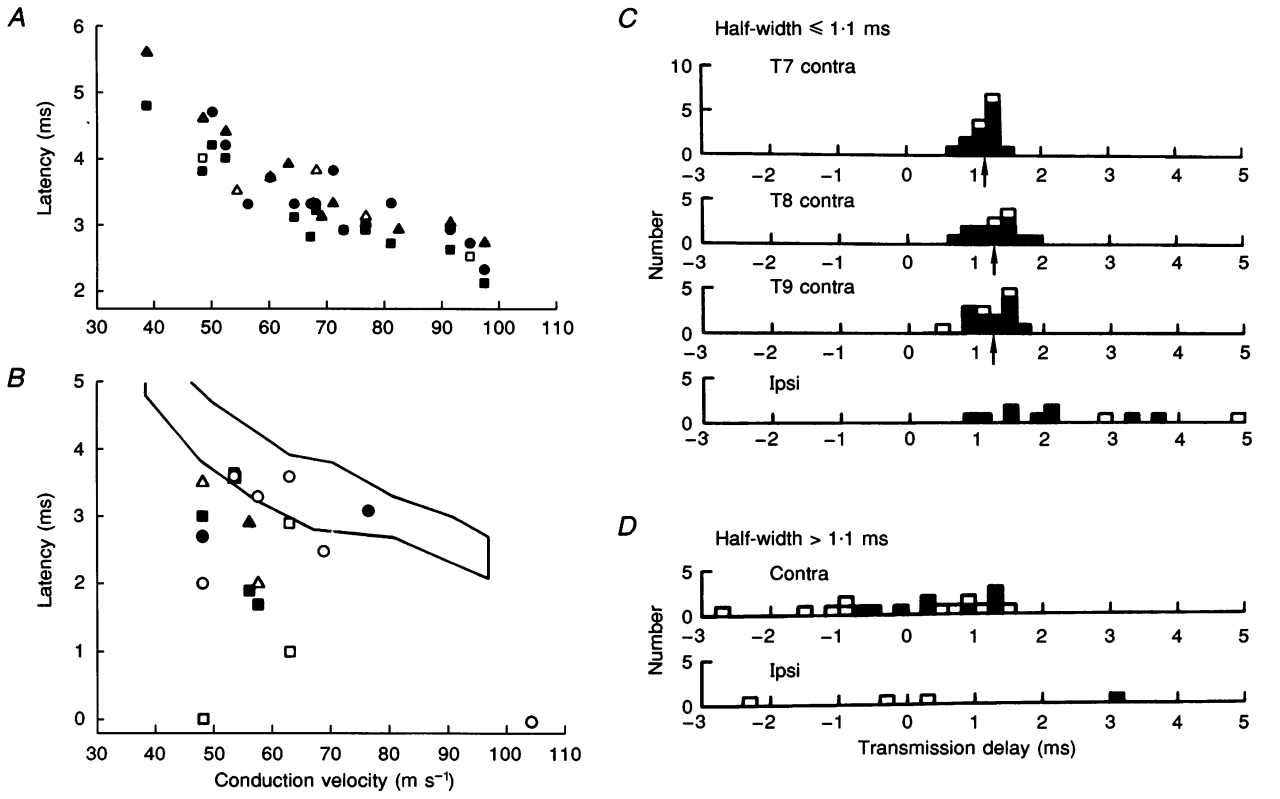

Figure 7. Timings of cross-correlation peaks

A, latencies of narrow peaks plotted against the conduction velocity of the reference unit. ■, T7; ●, T8; ▲, T9. Open symbols, non-significant peaks. *B*, similar plot for medium-width peaks. Same symbols as *A*. Region enclosed by lines is that occupied by the points in *A*. Only peaks involving contralateral nerves included in *A* and *B*. *C*, transmission delays for narrow peaks from the indicated segments (Contra, contralateral nerves) or all segments lumped together (Ipsi, ipsilateral nerves). Arrows indicate means for significant peaks. *D*, apparent transmission delays for medium-width peaks (segments lumped together for contralateral and for ipsilateral nerves, as indicated). In both *C* and *D*, ■ represents significant peaks; □, not significant.

as $k = 1{\cdot}0$ an overall mean was defined, with values 1·11 or 1·12 ($n = 58$ or $n = 33$). The histograms with relatively sharp medium-width peaks are best considered as 'non-tested' for the presence of narrow peaks, as in Davies *et al.* (1985*a*). Amplitudes of any narrow components within these peaks are impossible to assess, though they will not be very large: overall values of k for these medium-width peaks were between 1·07 and 1·15. The above values do not include data from the histograms from filament discharges. However the peak amplitudes from these histograms were in the same range (Fig. 8, ■).

For ipsilateral nerves both the mean of the individual values of k and the overall mean were less than for the contralateral nerves. Considering only the sampling level of mean count $\geqslant 121$, the mean k for significant peaks was 1·13 ($n = 9$), or 1·12 if the two non-significant peaks were included. The overall mean was 1·04 ($n = 32$).

Projection patterns revealed by spike-triggered averaging

The purpose of the spike-triggered averaging was to reveal more detail of the projections of the bulbospinal axons than could be revealed by the connections to expiratory motoneurones as shown in the correlation analysis. The basic properties of the recordings have already been described (Fig. 2*C* and *D*). In the ventral horn the waveforms that could be detected consisted of remote axonal potentials, TPs or FSPs.

General features of TPs and FSPs

TPs were distinguished from axonal potentials by their latency variation with position and by virtue of longer latencies than either the axonal potentials or the times of arrival of the axonal impulse as calculated from the collision test. They often showed a pronounced positive

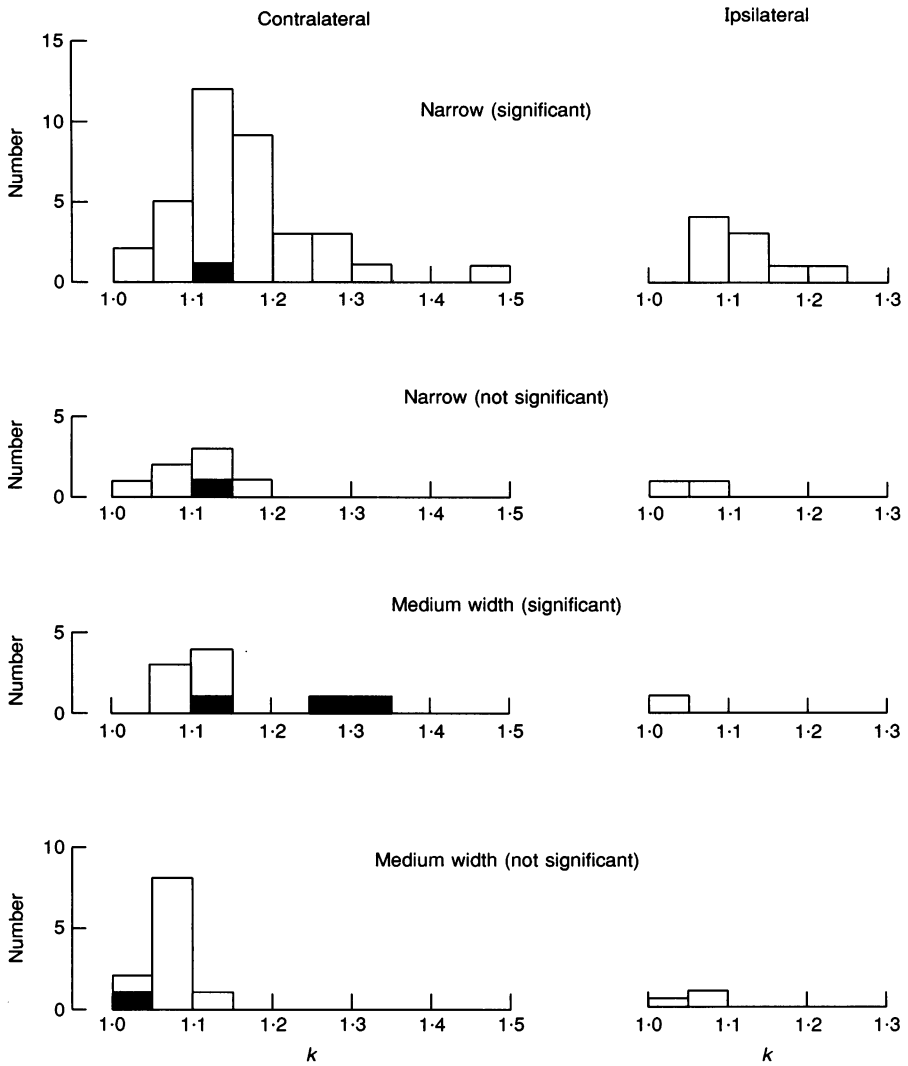

Figure 8. Distributions of k for the different categories of peaks

■, filament discharges.

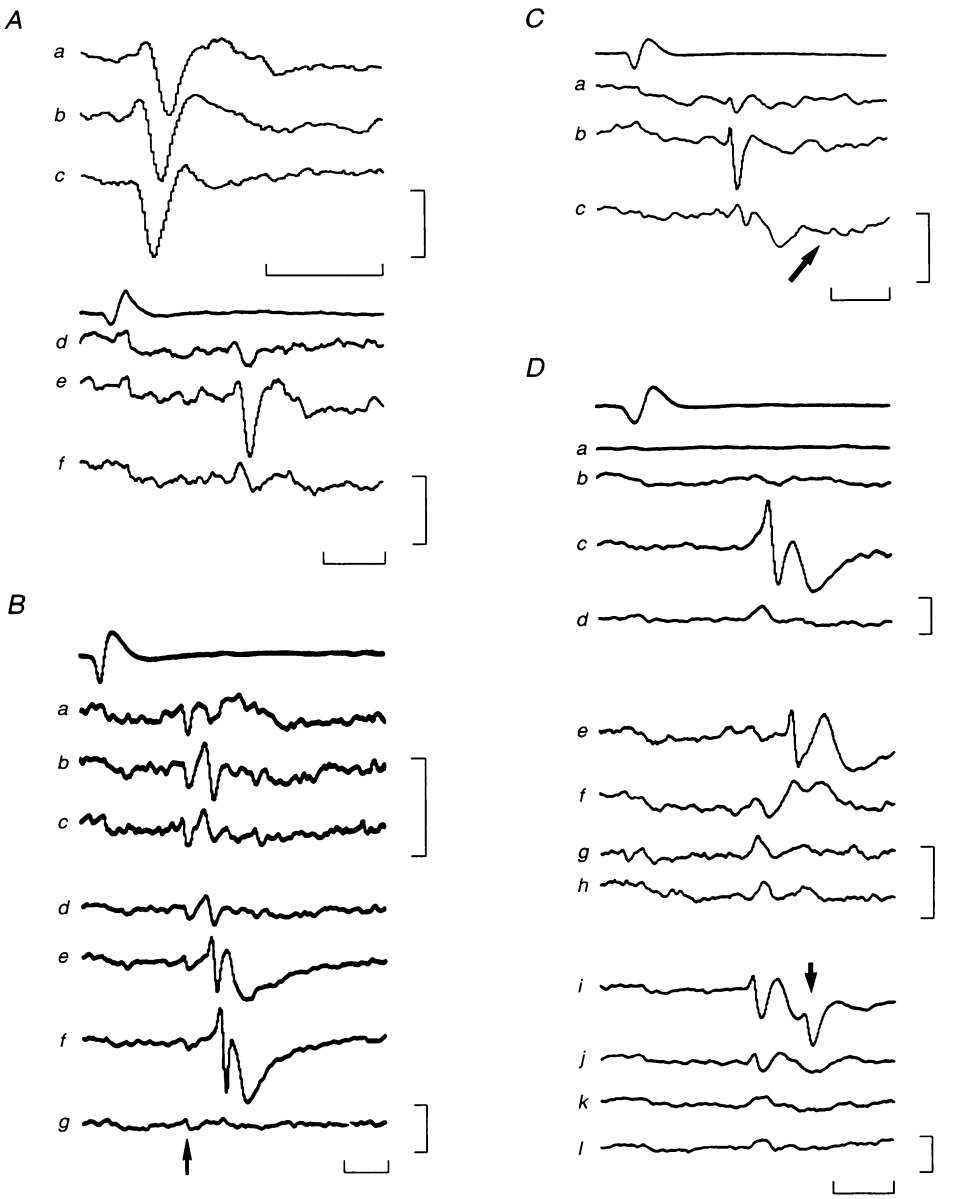

Figure 9. Examples of TPs and FSPs

Spike-triggered averages from four different trigger units are shown (panels *A–D*). *A*, a series of TPs (*a–c*) indicating a collateral conducting slowly, rostrally. The site for *b* was 0·2 mm caudal to that for *a*, the site for *c* was a further 0·2 mm caudal. In *a*, an FSP is also present, seen more clearly in *e*, which is the same average on a different time scale. *a–c* and *e*, all at 2·2 mm depth; *d* and *f*, on the same electrode track as *e* but 0·2 mm above and below, respectively. Trigger spike for *d–f* shown above *d*. *B*, a similar series to *A*, but indicating a collateral conducting caudally. *a–c*, averages at three sites on one track 3·05, 3·2 and 3·35 mm deep. *d*, the same as *b* at half the gain. *e–g*, averages at the same depth as *d* but 0·2, 0·4 and 0·6 mm caudal. Note: more widespread FSPs than in *A*; termination of collateral between sites of *f* and *g*; positive-going FSP at the edge of the synaptic focus (*a*); early, remote axon spike in all traces (arrow). *C*, an example of an FSP with a long-duration component, clear in *c* (arrow), just visible in *b*. Averages from three sites on one electrode track at depths 2·68, 2·88 and 3·13 mm for *a–c*, respectively. *D*, an extreme example of delayed TPs/FSPs at various latencies (all from one unit), including one complex TP, the second component of which is seen (superimposed on the earlier FSP) in *i* (arrow) and one positive-going FSP (*f*). Four averages at depths 2·35, 2·6, 2·85 and 3·1 mm (from above down in each case) on each of three electrode tracks: *a–d*, *e–h* (0·25 mm medial of *a–d*) and *i–l* (0·5 mm rostral of *e–h*). Top trace in each of *B*, *C* and *D*, is the trigger spike. Calibrations, 1 ms and 5 μV.

wave preceding a negativity, and only very occasionally a later positivity. TPs were usually of the simple form, at least as defined by Schmid, Kirkwood, Munson, Shen & Sears (1993). Only a few examples of complex TPs (i.e. TPs with multiple negative waves) were seen, excluding the occurrence of a remote axonal potential preceding the TP. The complex waveform in Fig. 2*Dc* is one of the exceptions (also see Fig. 9*Di*). Delays from the observed or calculated axonal time to the TP were mostly in the range 0·2–0·5 ms, but with a few at zero and a few up to 0·8 ms or, in one extreme case, 1·85 ms. Considerable variation in the delay for each unit was seen between different sites, even when close to each other (0·1–0·2 mm).

Delayed TPs are indicative of fine collaterals, whose geometry could sometimes be demonstrated directly, as in Fig. 9, where, for two units, these collaterals appeared to run parallel to the axon. For the unit of Fig. 9*A* the impulse travelled rostrally at about 3·3 m s^{-1} for 0·4 mm giving an FSP only at the most rostral site recorded, whereas for the unit of Fig. 9*B*, the impulse ran caudally at about 1·3 m s^{-1}, giving FSPs at two recording sites but terminating before the most caudal one. The conduction velocities of both collaterals were clearly different from their stem axons (76·7 and 67·1 m s^{-1}, respectively; cf. Shinoda, Yamaguchi & Futami, 1986). The axonal potential can be seen consistently at an earlier latency in *B* (arrow).

Figure 9 also shows typical FSPs. These were always preceded by TPs, 0·3–1·15 ms earlier. These delays cannot be taken directly as synaptic delays: one cannot be certain, given the slow conduction velocities of the collaterals, that the TP had been recorded at the site where the active synapses were located. However, the delays are entirely consistent with monosynaptic excitation (cf. Jankowska & Roberts, 1972). The shapes of the FSPs in Figs 2 and 9*A* and *B* are quite typical, though occasionally more complex shapes with a second (usually more slowly rising) negative component were present, as in Fig. 9*Cc* and *Di* (cf. Fig. 2*C*). On one occasion the origin of the second component was clear, as it was preceded by a second TP (Fig. 9*Di*). The latencies of TPs and FSPs for this unit showed a particularly wide variation between different sites (compare *Dc* with *De*). Overall, half-widths of FSPs, including any second component if more than 50% of the first in amplitude, ranged from 0·4 to 3·5 ms (mean ± S.D. 0·89 ± 0·40 ms, $n = 144$). All FSPs above 1 μV in amplitude were measured, from fourteen units. Only six FSPs (3 units) had half-widths longer than 1·5 ms.

Spatial distributions of FSPs were usually focal, often being restricted to 0·2–0·3 mm dorsoventrally, but sometimes spreading further rostrocaudally. Another regularly occurring (but by no means universal) feature was the occurrence of positive-going FSPs, most often found at the edge of a focus as in Fig. 9*Ba* and *Df*.

Amplitudes of TPs and FSPs

Spike-triggered averaging was used for a total of twenty units. TPs with FSPs were observed for eighteen of these, though the FSPs were only of small amplitude and positive-going for three of them. For the rostral part of T7 or T8 (0·4 mm rostral to 1 mm caudal of the most rostral dorsal root: see later) eighteen units were sampled (2–40 recording sites, median 12; 1–10 electrode tracks, median 3·5). TPs with FSPs were seen for sixteen of these units, FSPs from two of the units being positive-going. Maximum TP amplitudes ranged from 0·9 to 16·8 μV and maximum negative-going FSP amplitudes from 0·9 to 9·8 μV. Most of the units (14) were studied with a regularly spaced grid of points 0·25 mm apart (see later). For these (rostral T7 or T8), TPs with FSPs were seen for thirteen units (only positive-going FSPs for 2 of these). If further restriction is made to those units sampled on at least two electrode tracks and thus reasonably covering the whole ventral horn in one transverse plane, eight out of ten units gave TPs with negative-going FSPs and one unit (7 sites only) gave two small positive-going FSPs (TP amplitudes: maximum 0·9–7·2 μV, mean ± S.D. 4·36 ± 1·80, $n = 9$; FSP amplitudes: maximum 1·6–9·8 μV, mean ± S.D. 4·09 ± 2·55, $n = 8$). For six units, more closely spaced sampling was used near FSP foci, including 12–128 recording sites per unit (3–61 electrode tracks) giving maximum TP amplitudes of 5·3–16·8 μV (mean 10·5 μV, $n = 6$) and maximum FSP amplitudes of 2·4–10·0 μV (mean 5·8 μV, $n = 6$).

Spatial distributions of TPs and FSPs

For one unit in an early experiment an attempt was made to 'follow' individual collaterals (Fig. 9*A* came from this unit) and a large number of sites (128) were sampled on sixty-one electrode tracks (Fig. 10*A*). The sites were all within the ventral horn, as defined by measurements of motoneurone antidromic field potentials at a number of rostrocaudal positions. Several indications of collateral branching and foci of termination were identified by the form or timing of TPs and the presence of FSPs, including the only example (the only test) of TPs and FSPs contralateral to the descending axon (Fig. 10*E*). The most interesting observation was that large TPs and FSPs appeared to be restricted to rostral T8 and rostral T9 (Fig. 10*B* and *C*). In order to investigate this systematically for other units, formal comparisons were made between rostral and caudal sites using grids of recording sites which were spaced 0·25 mm apart, each grid consisting of two tracks per transverse plane, four sites per track. The grids were positioned so that the medial track was usually just lateral to the site of the largest antidromic motoneurone field potential from stimulating the dorsal ramus nerves and the lateral track through or just medial to the site of the largest field potential from the internal intercostal nerve (see Fig. 11*B* and Kirkwood *et al.* 1988). Grids at different rostrocaudal

levels were positioned (as far as possible) identically with respect to the field potential maxima (both for depth and mediolateral position), which were independently measured for each substantially different rostrocaudal level.

Eight units were tested with arrays of electrode tracks (different numbers of tracks, depending on the survival of the unit) at a rostral and a caudal position. One unit (tested with one rostral and one caudal grid) gave no TPs or FSPs and was one of the three units which gave no significant peaks in the cross-correlations (two segments tested on each side, the unit of Fig. 1*C*). Comparisons between rostral and caudal sites are thus restricted to seven units. The rostrocaudal positions of the rostral and caudal arrays of electrode tracks for each of the seven units are shown in Fig. 11*C*. The rostral array was always intended to be in the most rostral millimetre of the segment and the caudal array somewhere in the caudal half of the segment, the position of both being constrained somewhat by surface blood vessels. In one case (unit 03) the caudal array was in the segment above, rather than the caudal part of the same segment.

Figure 11*A* shows the averaged recordings at the sites illustrated in Fig. 11*B*. This set includes one of the largest

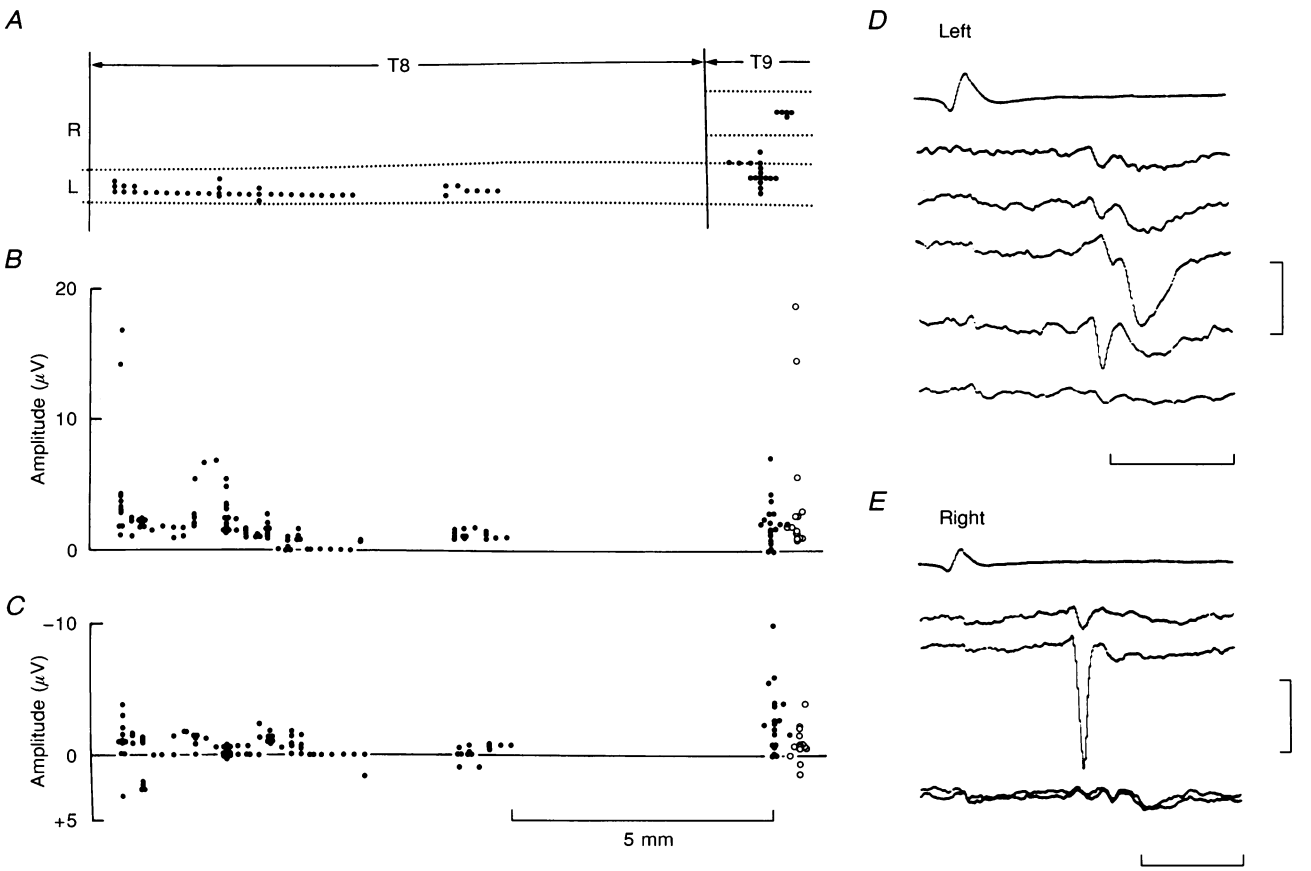

Figure 10. Spike-triggered averaging measurements at a large number of sites for one unit

A, schematic horizontal section through the ventral horn showing the location of tracks used for recording. Dotted lines show the medial and lateral borders of the ventral horn as indicated by motoneurone antidromic field potentials (internal intercostal nerves and dorsal ramus nerves of T8 or T9). Larger dots show the location of the electrode tracks. R, right; L, left. *B*, amplitudes of TPs (peak to peak) recorded on tracks at the corresponding rostrocaudal locations. *C*, similar plot for the FSPs, measured, with sign, from the baseline. Note negative-going FSPs shown above the axis. The largest FSPs (associated also with large TPs) seem to be most common at the rostral end of both T8 and T9. The few large TPs in *B* at about 2 mm caudal from the rostral end of T8 include those shown in Fig. 9 *a–c*. Open circles in *B* and C refer to averages from the right side of the cord. *D*, examples of averages measured in *B* and *C* (left side T9). Top trace, trigger spike; remainder, averages 0·1 mm apart on one track at depths 2·3–2·7 mm, bottom to top. *E*, examples as *D*, but from the left side. Top trace, trigger spike; next two averages, depths 2·8 and 2·9 mm, respectively on one track; lowest trace, two repeated averages superimposed at 2·8 mm depth, 0·1 mm caudal to the previous two averages. Calibrations, 2 ms and 10 μV.

TPs observed (recorded at the site arrowed), but otherwise is typical for the focal nature of the TP/FSP occurrences. Generally foci were not restricted to any part of the grid but were seen medially, laterally, dorsally or ventrally. Recordings from only one rostral and one caudal grid were achieved for this unit. No TPs or FSPs were seen on the caudal grid. A similar difference between rostral and caudal sites was present for each unit, though usually not so absolute. This is illustrated in Fig. 12, which shows histograms of FSP and TP amplitudes. TPs were measured peak to peak, FSPs baseline to peak, taking account of sign. Positive-going FSPs sometimes appeared on the same grid as negative-going FSPs, sometimes apparently concentrated in one grid, i.e. one rostrocaudal position. In Fig. 12*A* an example similar to that of Fig. 11*A*, with a very clear rostrocaudal difference, is shown and in *B* the unit with the least clear difference is illustrated. In this latter case there were the same number of negative-going FSPs of 1·0 μV or more in amplitude from both rostral and caudal arrays (7/24), but those in the rostral array were generally larger, so a rostrocaudal difference in the same direction was present for all seven units. Combined histograms of amplitude are shown in Fig. 12*C*, confirming this clear result. Both the numbers

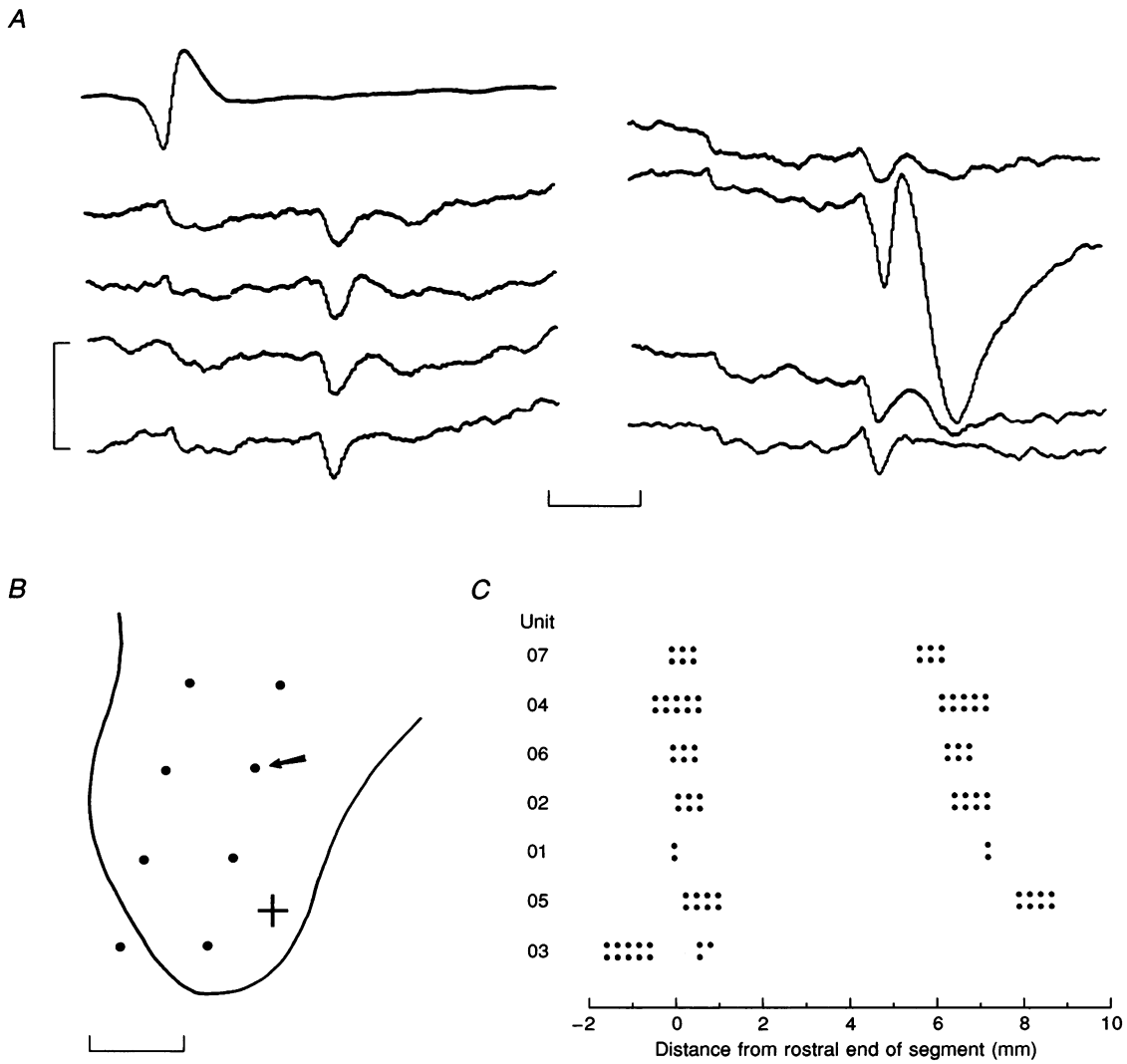

Figure 11. Systematic sampling for spike-triggered averaging

A, averages made at recording sites arranged in the grid illustrated in *B*. The grid was positioned with respect to the motoneurone antidromic field potentials; reference point indicated by the cross. Ventral horn outline schematic, as in Fig. 2. The layout of the averages in *A* corresponds to that of the sites in *B*, averages from the left track in *B* being shown on the left in *A*. The site with the largest FSP in *A* is arrowed in *B*. *C*, schematic dorsal view of the electrode tracks from the seven units in which systematic comparisons were made between grids of sites rostrally and caudally within a segment. Each point represents one track (four sites, as in *B*). At least one complete grid was made for each unit, rostrally and caudally. Length of a segment is usually 10–11 mm. Calibrations, 1 ms, 5 μV and 2·5 mm.

and sizes of TPs with amplitudes $\geqslant 1{\cdot}5\ \mu V$ and of FSPs with amplitudes $\geqslant 1{\cdot}0\ \mu V$ were larger for the rostral arrays than for the caudal ones.

The limits chosen for the above comparisons (1·5 or 1·0 μV) were derived from visual inspection of the baseline noise. This varied considerably from site to site depending on background activity (usually respiratory discharges). Sometimes FSPs could be detected below the chosen level of 1·0 μV, but not always reliably. FSPs above that level were considered to be, in general, reliably identified. The level for TPs (1·5 μV) is higher because the noise was generally 'spiky', therefore making identification of a TP, which has the same shape as the noise components, less safe than identification of a TP of the same amplitude.

Table 2 lists the numbers of TPs and FSPs with amplitudes greater than these values for the seven units tested and for the totals. From the totals, the fraction of sites with clear TPs rostrally (55/163) was highly significantly greater than that caudally (14/199; χ^2, $P < 0{\cdot}001$), as was the fraction of clear FSPs (58/163 *vs.* 21/199; χ^2, $P < 0{\cdot}001$). If only the first grid of eight sites (7 sites for one unit) for each rostral or caudal array was

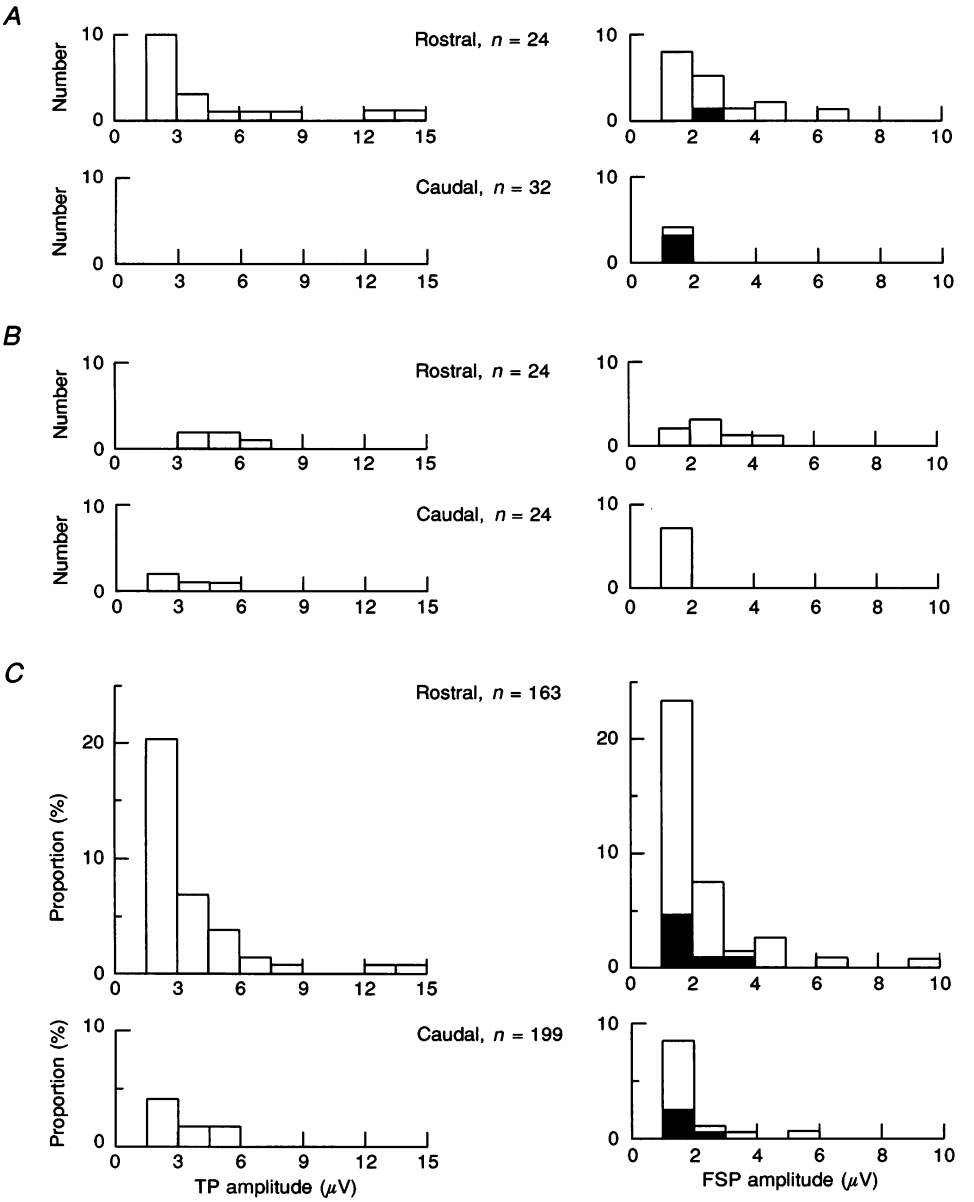

Figure 12. Comparisons of rostral and caudal sites within a segment

Distributions of amplitudes of TPs ($\geqslant 1{\cdot}5\ \mu V$) are shown on the left and FSPs ($\geqslant 1{\cdot}0\ \mu V$) on the right. In each case n gives the number of sites sampled. ■ represents positive-going FSPs. *A*, measurements from a unit showing a very clear rostrocaudal difference. *B*, measurements from another unit, where the difference is much less, but in the same direction. *C*, combined measurements from all the seven units shown in Fig. 11*C*.

included to give a more uniform sample, the rostrocaudal difference remained significant (TPs: 21/55 *vs.* 1/56, $P < 0{\cdot}001$; FSPs: 16/55 *vs.* 3/56, $P < 0{\cdot}01$).

Comparison with cross-correlations

Cross-correlations were performed for all ten units where rostral arrays of recording sites were tested for FSPs, using internal nerve discharges of the same segment (T7 or T8). Narrow peaks were identified in seven instances, one of these peaks being non-significant. The other three histograms either showed no peak or a non-significant one of medium width. These ten units fell neatly into two groups: five units for which k was less than 1·07 (mean ± S.D. 1·022 ± 0·028, taking absence of a narrow peak as $k = 1{\cdot}0$) and five units for which k was more than 1·15 (mean ± S.D. 1·207 ± 0·045, maximum 1·28). Combined histograms for TPs and FSPs for these two groups are shown in Fig. 13. Both TPs and FSPs were larger and more frequent for the group with higher values of k. The numbers of negative-going FSPs of amplitude at least 1·0 μV were 38/119 and 11/75 for the two groups, which are significantly different (χ^2, $P < 0{\cdot}05$). When positive-going FSPs were included, the proportions became 46/119 and 14/75, which are more significantly different ($P < 0{\cdot}01$). The proportions of TPs of at least 1·5 μV amplitude were also highly significantly different (46/119 *vs.* 10/75, $P < 0{\cdot}001$). If only the first grid for each unit was included, the differences remained significant (FSPs: 15/40 *vs.* 4/39, $P < 0{\cdot}05$; TPs: 18/40 *vs.* 3/39, $P < 0{\cdot}001$).

Thus the units with stronger connections to the expiratory motoneurones gave larger and/or more widespread synaptic connections in the rostral millimetre of the segment. However, it is worth noting that the units giving stronger connections to the segment of interest did not necessarily give strong connections overall. The five units giving the strong connections were tested in another one or two contralateral segments each, giving nine additional histograms in all. Excluding two significant medium-width peaks, but including one non-significant medium-width peak as $k = 1{\cdot}0$, the mean k was 1·106 (± 0·065 (S.D.), $n = 7$). The comparable figures from the five weaker connections (8 histograms, one significant medium-width peak excluded) were hardly less: 1·087 (± 0·065 (S.D.), $n = 7$).

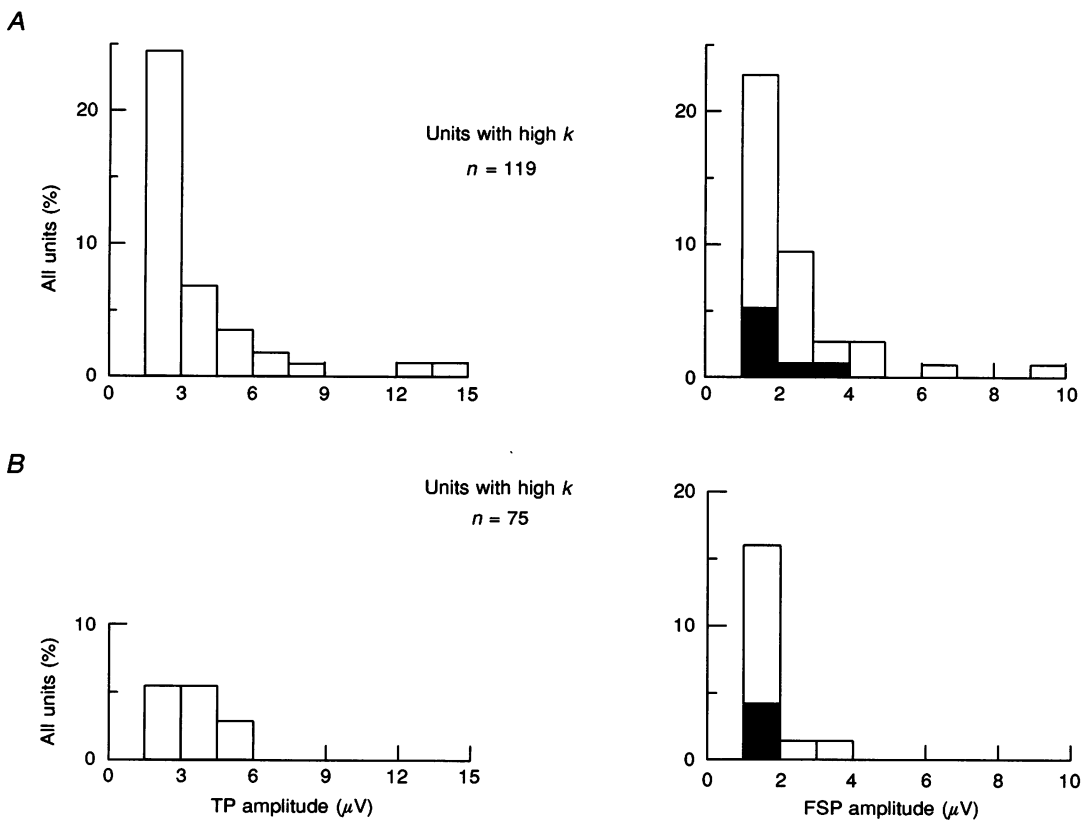

Figure 13. Comparisons of spike-triggered averaging measurements for units with strong connections *vs.* units with weak connections as shown in the cross-correlations

Combined distributions of amplitudes of TPs ($\geqslant 1{\cdot}5$ μV) and FSPs ($\geqslant 1{\cdot}0$ μV) for sites on complete rostral grids. In each case n gives the number of sites sampled. ■ represents positive-going FSPs. *A*, five units where k was > 1·15 in the cross-correlation with the internal intercostal nerve of the same segment; *B*, five units where k was < 1·07.

Table 2. Proportion of sites for each unit which gave TPs with amplitudes ≥ 1·5 μV or FSPs with amplitudes ≥ 1·0 μV

	Rostral arrays				Caudal arrays			
	TP		FSP		TP		FSP	
Unit (segment)	Sites	%	Sites	%	Sites	%	Sites	%
01 (T7)	8/8	100	3/8	38	0/8	0	0/8	0
02 (T8)	18/24	75	17/24	67	0/32	0	4/32	13
03 (T7/8)	5/12	42	2/12	17	1/39	3	1/39	3
04 (T8)	14/40	35	17/40	43	6/40	15	5/40	13
05 (T8)	4/32	13	9/32	28	2/32	6	3/32	9
06 (T7)	1/23	4	3/23	13	1/24	4	1/24	4
07 (T7)	5/24	21	7/24	29	4/24	17	7/24	29
Total	55/163	34	58/163	36	14/199	7	21/199	11

Positive-going FSPs (20 % of the total) are included. Unit identifications correspond to Fig. 11*C*.

DISCUSSION

The results show that cross-correlation peaks interpreted here as indicating monosynaptic connections are common between expiratory bulbospinal neurones and the expiratory motoneurones which give efferent discharges in thoracic nerves. This is in agreement with Cohen *et al.* (1985) but apparently in disagreement with Merrill & Lipski (1987). It is therefore important to discuss the certainty of the identification of these direct connections before attempting to estimate, in functional terms, how strong the connections are.

Identification of connections

The identifications depend on both the timings and the half-widths of the observed peaks. As in Davies *et al.* (1985*a*, *b*), the crucial measurement for timing is the conduction velocity, or more accurately, the orthodromic conduction time for each unit. The measurements here involving spike-triggered averages of axonal potentials serve to validate fully the method of using 0·5 ms less than the critical delay in the collision test (at twice threshold) as a measure of the conduction time to the stimulating electrodes. The very close agreement between the two measurements in Fig. 3*A*, over a wide range of conduction times, shows that this single-point method is as accurate as the double-point stimulation used by Dick & Berger (1985), and much more accurate than most single-point methods relying on measurements of antidromic conduction time, which must involve two assumptions: a utilization time and a value for a delayed antidromic soma invasion time.

The mean conduction velocity here is higher than in most previous reports (Monteau & Hilaire, 1991) including that in Merrill & Lipski (1987), but the conduction velocities they measured (as they admit) could be too low because of stimulation of collaterals rather than stem axons. There may be a slight bias here because the slowest firing neurones were generally ignored, being unsuitable for the cross-correlations, but these rejected neurones represented a small proportion of those encountered.

The values of transmission time for the narrow cross-correlation peaks (means 1·17–1·29 ms for the different segments, Fig. 7*C*) are slightly less than for the inspiratory axons of Davies *et al.* (1985*a*) (1·54 or 1·47 ms). One component of this time, the peripheral conduction time, should be very similar for the inspiratory and expiratory cases. Thus the difference is most likely to arise as a different degree of slowing in preterminal axonal branches, the transmission times here being entirely consistent with the observed timings of the TPs and FSPs, the variation in which is also appropriate to explain the spread in the transmission time distributions.

Thus the timings of the narrow peaks are entirely consistent with monosynaptic excitation of the contralateral motoneurones by the bulbospinal neurones. The confirmation of the accuracy of the conduction time estimations here and the similarity of the transmission times here and in Davies *et al.* (1985*a*; despite the small difference mentioned above) further confirms the similar conclusion in that earlier paper.

In contrast, the latencies of the medium-width peaks here generally did not correspond to the latencies expected for a monosynaptic connection, most of them being too short (Fig. 7*B* and *D*) and these peaks must therefore have arisen by presynaptic synchronization, probably in the medulla, as was hypothesized for inspiratory neurones by Davies *et al.* (1985*a*), whose model should be consulted for a fuller explanation. The distinction is demonstrated more clearly here than in Davies *et al.* (1985*a*) because here both the latencies and the half-widths of the medium-width peaks could be measured more easily. In Davies *et al.* (1985*a*) many of these peaks were obscured by HFO, which is a periodic feature with a period of about 10 ms.

The overall distribution of half-widths of the peaks (Fig. 6) is unimodal and it might seem, especially given the appearance of some of the histograms with half-widths near to the dividing line for narrow *vs.* medium widths (e.g. Figs 4*H* and 5*B*), that this half-width dividing line of 1·1 ms is rather arbitrary. However, the clear difference in latency distributions (Fig. 7) suggests that it is about right: none of the narrow peaks had unduly short latencies, whereas most of the medium-width peaks did. A few medium-width peaks with latencies appropriate to a monosynaptic connection would be expected: at least *some* of the bulbospinal neurones assumed to be synchronized in the medulla would happen by chance to have the appropriate timing within this synchronization to give this latency.

It should be emphasized that the value of 1·1 ms for the dividing line is only coincidentally the same as in Davies *et al.* (1985*a*) and represents the minimum half-width of peaks that are likely from synchronization (itself of very short duration) of bulbospinal units in the medulla which have conduction velocities covering the whole range found here. The range of half-widths observed (mostly above this limit), is likely to represent the range of durations for that synchronization within the medulla. For the thoracic nerve recordings in Davies *et al.* (1985*a*) there were no peaks with half-widths in the range 1·1–1·7 ms. This fits well with the model assumed, there being greater temporal dispersion in the slower population of inspiratory bulbospinal axons than the expiratory bulbospinal axons here (the 1·1 ms criterion being derived in Davies *et al.* (1985*a*) for the conduction distance to the phrenic motor nucleus). The main peak in the half-width distribution there, however, was very similar for the phrenic and for the thoracic levels and very similar to Fig. 6 here, with a modal value around 0·5–0·7 ms and including half-widths up to 1·1 ms. Thus a half-width up to 1·1 ms still seems, empirically, to be a good description of a peak arising from monosynaptic connections to these small multiunit populations of either inspiratory or expiratory motoneurones. Davies *et al.* (1985*a*) pointed out for the inspiratory axons that if a conduction distance shorter than that from the medulla to C5 was involved, peaks due to monosynaptic connections could not be distinguished from those resulting from presynaptic synchrony. Similarly, for the expiratory axons in this study, where the conduction velocities are faster, a conduction distance any shorter than we happened to use (medulla to T7) would also lead to ambiguity.

Of course a degree of uncertainty will always remain for any individual peak, but for the reasons explained above, the number of false positives in the population of peaks taken as a whole is probably well balanced by false negatives. There will also be a certain amount of contamination, i.e. some components due to presynaptic synchronization will be present in otherwise unambiguous narrow peaks. Mostly, however, the shapes of the peaks suggest that this contamination will be small. In estimating the strengths of the connections via the amplitude measurement k, as opposed to an area measurement (cf. Cope, Fetz & Matsumura, 1987), the effects of such contaminating components are minimized. The use of a narrow bin width reduces the dependence of k upon the bin width and the use of large numbers of counts in the histograms reduces the effects of noise on the measurement of k.

A contribution from a disynaptic link to some of the peaks also cannot be totally ruled out. The rather broad base on peaks such as those in Figs 4*G* or 5*B* could be equally likely to arise from this or from presynaptic synchronization. The effect on the main population is likely to be small for the same reasons as in Davies *et al.* (1985*a*). In the measures of strength of connection discussed below, any effect will again be minimized by measuring the amplitude of the peak rather than an area. The maximum nearly always occurred early in the peak, too early to be affected by a disynaptic component.

Thus it is safe to conclude that, in general, the narrow peaks for contralateral motoneurones represent a monosynaptic connection. Further, the distributions of half-widths and latencies for the peaks from ipsilateral correlations are sufficiently close to those from the contralateral motoneurones for there to be no doubt that these narrow peaks also represent a monosynaptic link and that many of the bulbospinal neurones must give axon collaterals which re-cross the mid-line to synapse on motoneurones on the same side as the bulbospinal somata. Although contrary to observations of Merrill & Lipski (1987) this conclusion is consistent with the results of Cohen *et al.* (1985) and is supported by the recordings from the one unit tested here with extracellular spike-triggered averaging. This gave a TP that was large and clear and of such a short duration (Fig. 10*E*) that it could only represent the direct projection of that unit.

The correlation results confirm directly the generally accepted view that the expiratory bulbospinal neurones of the caudal ventral respiratory group are all excitatory. The only exceptions could be the four units where connections were not positively confirmed. The occurrence of largely negative-going FSPs supports this general conclusion. Moreover, the units giving only positive-going FSPs also gave excitation in the cross-correlations, so the positive-going FSPs do not represent focal outward synaptic currents of inhibition, but probably outward currents at one site on the target neurones, consequent on inward currents resulting from excitation elsewhere on these neurones (Taylor, Stephens, Somjen, Appenteng & O'Donovan, 1977; Kirkwood, Schmid, Otto & Sears, 1991; Kirkwood, Schmid & Sears, 1993).

Strength of connections

The certainty of the identification expressed above allows the strength of the monosynaptic connection to be assessed. This connection (Table 1, Fig. 8) must be regarded as strong. Although the mean amplitude of the narrow peaks for nerves contralateral to the cell somata ($k = 1{\cdot}15$) was only slightly more than that for either the external (inspiratory) intercostal or the phrenic nerve ($k = 1{\cdot}11$) in Davies *et al.* (1985*b*), the proportion of histograms showing a peak was much greater (41/65) than for the external intercostals (50/295) and somewhat greater than for the phrenic nerve (13/27). The overall mean for k (absent peaks taken as $k = 1{\cdot}0$) is thus 1·11 in this study, compared with 1·02 or 1·06 for the inspiratory intercostals or phrenic nerve, respectively. Thus, when measured by an identical method, the connections here are nearly twice as strong as those from bulbospinal inspiratory neurones to phrenic motoneurones, themselves generally regarded as representing a substantial input (Monteau & Hilaire, 1991).

Davies *et al.* (1985*b*) also made approximate calculations for the amount of depolarization in the motoneurones derived from these connections, assuming first that k of 1·5 represented an EPSP of 100 μV amplitude and that EPSPs summed linearly, second that the measured firing rates represented those of the population as a whole, and third that there were about 400 inspiratory bulbospinal neurones on each side of the medulla. The same assumptions can be made here. The first was further justified by Kirkwood & Sears (1991) and gives the mean EPSP size here as $100\ \mu\text{V} \times 0{\cdot}11/0{\cdot}5 = 22\ \mu\text{V}$. For the second, the mean firing rate here was almost the same as in Davies *et al.* (1985*b*; 107 *vs.* 99 impulses s^{-1}) and for the third, it should be noted that the number of expiratory bulbospinal neurones is likely to be similar to the number of inspiratory bulbospinal neurones (a longer column of cells in the ventral respiratory group than for the inspiratory respiratory group but none in the dorsal group). Merrill & Lipski (1987) suggest 700 as the number of expiratory neurones, so the assumption here is a conservative one. Thus, whereas the monosynaptically derived depolarization for phrenic motoneurones was calculated as 3–4 mV, here it should be 7–8 mV. In addition, from the ipsilateral bulbospinal neurones (collaterals re-crossing the cord), where the overall mean k was 1·04, another 2·5 mV should be added. This gives a total of about 10 mV, i.e. about two-thirds of that required to depolarize a motoneurone from a notional resting potential of −70 mV to a firing threshold of −55 mV.

These calculations are very approximate. Neither non-linear (shunting) addition of EPSPs, (which would reduce their effectiveness) nor the turning on of voltage-sensitive membrane channels (which could amplify the effectiveness of the EPSPs) has been taken into account. However, even if the estimation is accurate only to within an order of magnitude, when considered together with the comparisons with the phrenic motoneurones, it must lead to the conclusion that the monosynaptic input here is a substantial one and it may well be the main one determining the outputs of these motoneurones.

These results are consistent with those of Cohen *et al.* (1985) for the proportion of units giving clear peaks in their cross-correlations, for both the contra- and ipsilateral connections. What is new here is the certainty of identification of the monosynaptic component and the estimation of its strength. The only feature not represented here is the 34% of units in Cohen *et al.* (1985) that were defined as 'step-ramp' in firing pattern and which gave very few connections. The units in Cohen *et al.* (1985) were tested in decerebrate animals with a cycle-triggered pump and a pneumothorax, so it may be no surprise that such a category of units were not seen here. However, nearly all the units here (89%) showed *some* connections, so the present measurements give little support to the view that there is a category of units which do not participate in the pathway. The only possibility is that the two strongly pump-sensitive units here, which did not give a connection, could correspond to this category.

The results are apparently completely inconsistent with those of Merrill & Lipski (1987) from intracellular spike-triggered averaging, which indicated an exceptionally weak connection, comprising two EPSPs (55 and 62 μV) in fifty-seven trials and a mean EPSP size of 2·05 μV, compared with the 22 μV here. This contrasts with results for both the external intercostal and the phrenic motoneurones for which cross-correlation measurements and spike-triggered average EPSP measurements were in reasonable agreement (Davies *et al.* 1985*b*).

How could this difference arise? The methods were identical for both types of motoneurone in each type of study. Moreover, the difference between the results here and Merrill & Lipski (1987) are unlikely to have arisen by chance. The 22 μV here corresponds to a connectivity of twenty-one out of fifty-seven EPSPs if they were all about 59 μV in amplitude. Twenty-one out of fifty-seven is very significantly different from two out of fifty-seven (χ^2 test, $P < 0{\cdot}001$). Even half of this (10/57) is still significantly different from two out of fifty-seven ($P < 0{\cdot}05$). The conclusion therefore is that the two methods have measured two different populations of expiratory connections. The most obvious way for this to come about is for these two populations to represent two different motoneurone samples. This could arise because the selection criteria were different. If it *is* the case that only some motoneurones receive this input, which the calculations above suggest is nearly enough to bring them to threshold, then this population will automatically be those which are first recruited, and thus it comprises the

motoneurones most likely to be sampled in the cross-correlations. In contrast, the intracellular measurements will give a much more even sample.

The simplest hypothesis to explain the results is thus that a population comprising about 10% of the expiratory motoneurones with axons in the internal intercostal nerve are specialized to receive the monosynaptic bulbospinal expiratory input. This would not be inconsistent with the general pattern of the output. The internal intercostal nerve is a relatively thick nerve and the observed discharges could easily represent only 10% of the potentially expiratory axons being active. The total number of α-motoneurone axons is typically 300–400 (Sears, 1964*a*), of which some (say 30%) could be inspiratory, giving the necessary 10% as about twenty-five axons, which is easily sufficient to give the measured impulse rates. Merrill & Lipski (1987) stated that only 44% of their motoneurones showed respiratory drive potentials, and with a mean amplitude of only 3·7 mV for this and a maximum below 10 mV, most of these would not reach threshold. This is consistent with the fact of most of their motoneurones not being in the same population as was sampled in the cross-correlations.

Functional considerations

It is of obvious interest which motoneurones are represented in the 10% which are hypothesized above to be specialized to receive the monosynaptic input. One possibility is that they represent only *one* of the muscles innervated by the internal intercostal nerve. Such an explanation would be equivalent to the hypothesis of Kirkwood & Sears (1989; also see Vaughan & Kirkwood, 1993) that for rostral segments the descending connection to the inspiratory motoneurones with axons in the internal intercostal nerves is more direct than that to motoneurones with axons in the external nerve. At least four muscles with expiratory actions are innervated from the internal intercostal nerve in the segments used here: internal intercostal, external abdominal oblique, transversus abdominis and rectus abdominis. Preliminary evidence suggests that a restriction of the projection to motoneurones of only one muscle is certainly not absolute, because motoneurones of at least two of the above muscles definitely receive the projection (Road & Kirkwood, 1993). However, the projection could nevertheless be unequal, as in the apparently weaker connections here to the filaments (i.e. to the internal intercostal muscle) than to the nerve as a whole.

An alternative explanation, not necessarily exclusive to that above, is that the connections are spatially restricted within each segment, corresponding to the observed spatial restrictions in the distributions of TPs and FSPs. This explanation would fit well with the apparent ease of finding spike-triggered average EPSPs by Kirkwood & Sears (1973). Although the rostrocaudal locations of the motoneurones within the segment were not recorded in those early experiments, it was certainly our practice in the laboratory at that time at least to start searching for motoneurones at the rostral end of the segment, where the yield of respiratory motoneurones (both inspiratory and expiratory) seemed to be best. The largely negative results of Merrill & Lipski (1987) would then be assumed to result from their making recordings mostly elsewhere in the segments. Again, however, such an explanation would not be expected to be absolute. Though smaller or less frequent than rostrally, TPs and FSPs were not totally absent from recordings at caudal sites.

Both these explanations are speculative. The functional reasons why either should occur are even more so. The expiratory muscles participate in many different actions. Pairs of muscles which may be synergistically active (i.e. in phase) in some actions may be antagonistically active in others, e.g. vomiting *vs.* respiration (McCarthy & Borison, 1974). Depending on how the expiratory bulbospinal neurones behave in these different actions (Price & Batsel, 1970; Jakuš, Tomori & Strańsky, 1985; Miller, Tan & Suzuki, 1987) it may be most convenient for their actions to be gated at spinal level and therefore mostly controlled via interneurones. The 10% of motoneurones which were hypothesized above to be specialized for the monosynaptic input during respiration could still represent an area (or areas) of muscles which are always active whenever *most* of the bulbospinal neurones are *simultaneously* active, as in the CO_2-stimulated respiration used here.

It should be noted that this does not mean that even these motoneurones cannot be selectively recruited for other motor acts. For instance, in fictive vomiting, Miller *et al.* (1987) showed that bulbospinal neurones, as a whole, did not increase their firing rates from levels seen in normocapnic respiration and, moreover, did not all fire in the same phases of vomiting. About two out of three fired in phase with intercostal motoneurones, and one out of three during the opposite phase when abdominal motoneurones were active. Thus, even if a monosynaptic connection did exist from nearly all bulbospinal neurones to the motoneurones of a given muscle (as suggested above) and that muscle was 'intended' to be active during the firing of only one of the two groups of bulbospinal neurones, then the required pattern of output *could* still occur. Motoneurone discharges during the opposite phase, when an output is not required, need not occur, despite the monosynaptic excitation at this time, because with only a proportion of the bulbospinal input active there would generally be insufficient depolarization to reach threshold. However, some of the variability which may sometimes be seen in an otherwise clear pattern (Miller & Yates, 1993) could still sometimes occur by this route. The discharges during the 'required' phase would be expected to occur with the support of interneurones.

This explanation would be consistent with the normally low level of expiratory discharge seen in well-anaesthetized normocapnic animals. In order to get significant discharges (assuming vomiting, etc. is not evoked) either the bulbospinal neurones need to be strongly concurrently active (as here) or interneurones need to be activated, for instance with lighter anaesthesia or spinal lesions (cf. Kirkwood, Sears, Tuck & Westgaard, 1982; Kirkwood, Sears & Westgaard, 1984). Plenty of expiratory interneurones exist (Kirkwood *et al.* 1988; Bellingham & Lipski, 1990; Grélot, Milano, Portillo & Miller, 1993), many of them excitatory (Kirkwood *et al.* 1993). If those at the cervical level are typical (Grélot *et al.* 1993) they will show a wide variety of patterns in the various motor actions of the respiratory motoneurones. Thus, despite the emphasis here on the monosynaptic input being largely responsible for the motor output under the particular conditions used in the present experiments, the generalities put forward by Davies *et al.* (1985*b*) about interneuronal inputs being the main determinant of respiratory motoneurone output will be just as valid for expiratory discharges (in most conditions) as they were for inspiratory ones.

Anatomical considerations

A considerable amount of anatomical information about the axon collaterals can be derived from the TPs and FSPs. The occurrence of some large TPs, delayed from the axon spike but with the occurrence of FSPs being more spatially restricted and with the general absence of complex TPs (cf. the common occurrence of these for some types of interneurones in Kirkwood *et al.* 1993), suggests the presence of fine collaterals, sometimes extending for half a millimetre or more, but not highly branched. The TPs in Fig. 10*E*, together with the correlation results, indicate that some collaterals cross the mid-line. It seems likely that these are restricted to the rostral part of a segment, so it is not surprising that they were not observed by Merrill & Lipski (1987). The widespread locations of the TPs and FSPs do not help in identifying the targets of the collaterals. These could be either motoneurones or interneurones, but the correlation between the occurrence of both TPs and FSPs and the strength of the connections to the motoneurones (Fig. 13) suggest that the projections to the motoneurones represent a relatively high proportion of the total.

There remains the intriguing question of why the collaterals appear to be directed preferentially to the rostral part of the segment. If they are directed to particular target motoneurones (presumably those whose discharges were recorded) the question would still remain as to why these particular motoneurones were located there. Alternatively, if particular target interneurones were located there, this could represent a stereotyped rostrocaudal pattern of function within the segment, although preliminary evidence from the rostrocaudal distribution of interneurones with different firing patterns (J. Brunneman, C. Vaughan & P. A. Kirkwood, unpublished observations) is not hopeful in this regard. Finally, it could be simply a developmental epiphenomenon, but nevertheless of interest: is there a marker laid down during development which promotes the growth of collaterals at this location, or does the adult pattern arise by the elimination of branches from a more diffuse pattern? Whatever the reasons turn out to be, the apparently stereotyped anatomy of the axon collaterals suggested here, combined with the stereotyped patterns of activity under anaesthesia, could combine to make these axons good candidates for future studies of plasticity or development.

Bellingham, M. C. & Lipski, J. (1990). Respiratory interneurons in the C5 segment of the spinal cord of the cat. *Brain Research* **533**, 141–146.

Cohen, M. I., Feldman, J. L. & Sommer, D. (1985). Caudal medullary expiratory neurone and internal intercostal nerve discharges in the cat: effects of lung inflation. *Journal of Physiology* **368**, 147–178.

Cope, T. C., Fetz, E. E. & Matsumura, M. (1987). Cross-correlation assessment of synaptic strength of single Ia fibre connections with triceps surae motoneurones in cats. *Journal of Physiology* **390**, 161–188.

Davies, J. G. McF., Kirkwood, P. A. & Sears, T. A. (1985*a*). The detection of monosynaptic connexions from inspiratory bulbospinal neurones to inspiratory motoneurones in the cat. *Journal of Physiology* **368**, 33–62.

Davies, J. G. McF., Kirkwood, P. A. & Sears, T. A. (1985*b*). The distribution of monosynaptic connexions from inspiratory bulbospinal neurones to inspiratory motoneurones in the cat. *Journal of Physiology* **368**, 63–87.

Davies, R. O. & Kubin, L. (1986). Projection of pulmonary rapidly adapting receptors to the medulla of the cat: an antidromic mapping study. *Journal of Physiology* **373**, 63–86.

Dick, T. E. & Berger, A. J. (1985). Axonal projections of single bulbospinal inspiratory neurons revealed by spike-triggered averaging and antidromic activation. *Journal of Neurophysiology* **53**, 1590–1603.

Dick, T. E., Viana, F. & Berger, A. J. (1988). Electrophysiological determination of the axonal projections of single dorsal respiratory group neurons to the cervical spinal cord of the cat. *Brain Research* **454**, 31–39.

Grélot, L., Milano, S., Portillo, F. & Miller, A. D. (1993). Respiratory interneurons of the lower cervical (C4–C5) cord: membrane potential changes during fictive coughing, vomiting, and swallowing in the decerebrate cat. *Pflügers Archiv* **425**, 313–320.

Jakuš, J., Tomori, Z. & Strańsky, A. (1985). Activity of bulbar respiratory neurones during cough and other respiratory tract reflexes in cats. *Physiologia Bohemoslovaca* **34**, 127–136.

Jankowska, E. & Roberts, W. J. (1972). Synaptic actions of interneurones mediating reciprocal Ia inhibition of motoneurones *Journal of Physiology* **222**, 623–642.

Kirkwood, P. A. (1990). Synaptic connections in the thoracic spinal cord from expiratory bulbospinal neurones in the anaesthetized cat. *Journal of Physiology* **430**, 56*P*.

KIRKWOOD, P. A., MUNSON, J. B., SEARS, T. A. & WESTGAARD, R. H. (1988). Respiratory interneurones in the thoracic spinal cord of the cat. *Journal of Physiology* **395**, 161–192.

KIRKWOOD, P. A., SCHMID, K., OTTO, M. & SEARS, T. A. (1991). Focal blockade of single unit synaptic transmission by iontophoresis of antagonists. *NeuroReport* **2**, 185–188.

KIRKWOOD, P. A., SCHMID, K. & SEARS, T. A. (1993). Functional identities of thoracic respiratory interneurones in the cat. *Journal of Physiology* **461**, 667–687.

KIRKWOOD, P. A. & SEARS, T. A. (1973). Monosynaptic excitation of thoracic expiratory motoneurones from lateral respiratory neurones in the medulla of the cat. *Journal of Physiology* **234**, 87–89*P*.

KIRKWOOD, P. A. & SEARS, T. A. (1989). Dual descending pathways to inspiratory motoneurones in the anaesthetized cat. *Journal of Physiology* **414**, 15*P*.

KIRKWOOD, P. A., SEARS, T. A., TUCK, D. L. & WESTGAARD, R. H. (1982). Variations in the time course of the synchronization of intercostal motoneurones in the cat. *Journal of Physiology* **327**, 105–135.

KIRKWWOD, P. A., SEARS, T. A. & WESTGAARD, R. H. (1984). Restoration of function in external intercostal motoneurones of the cat following partial central deafferentation. *Journal of Physiology* **350**, 225–251.

MCCARTHY, L. E. & BORISON, H. L. (1974). Respiratory mechanics of vomiting in decerebrate cats. *American Journal of Physiology* **226**, 738–748.

MERRILL, E. G. (1973). The descending pathways from the lateral respiratory neurones in cats. *Journal of Physiology* **218**, 82–83*P*.

MERRILL, E. G. & AINSWORTH, A. (1972). Glass-coated platinum-plated tungsten microelectrodes. *Medical and Biological Engineering* **10**, 662–672.

MERRILL, E. G. & LIPSKI, J. (1987). Inputs to intercostal motoneurons from ventrolateral medullary respiratory neurons in the cat. *Journal of Neurophysiology* **57**, 1837–1853.

MILLER, A. D., TAN, L. K. & SUZUKI, I. (1987). Control of abdominal and expiratory intercostal muscle activity during vomiting: role of ventral respiratory group expiratory group neurons. *Journal of Neurophysiology* **57**, 1854–1866.

MILLER, A. D. & YATES, B. J. (1993). Evaluation of role of upper cervical inspiratory neurons in respiration, emesis and cough. *Brain Research* **606**, 143–147.

MONTEAU, R. & HILAIRE, G. (1991). Spinal respiratory motoneurons. *Progress in Neurobiology* **37**, 83–141.

MOORE, G. P., SEGUNDO, J. P., PERKEL, D. H. & LEVITAN, H. (1970). Statistical signs of synaptic interaction in neurons. *Biophysical Journal* **10**, 876–900.

MUNSON, J. B. & SYPERT, G. W. (1979). Properties of single central Ia fibres projecting to motoneurones. *Journal of Physiology* **296**, 315–328.

PORTER, R. & LEMON, R. N. (1993). *Corticospinal Function and Voluntary Movement*. Oxford University Press, Oxford.

PRICE, W. M. & BATSEL, H. L. (1970). Respiratory neurons participating in sneeze and in response to resistance to expiration. *Experimental Neurology* **29**, 554–570.

RICHTER, D. W. & BALLANTYNE, D. (1983). A three phase theory about the basic respiratory pattern generator. In *Central Neurone Environment*, ed. SCHLÄFKE, M. E., KOEPCHEN, H. P. & SEE, W. R., pp. 164–174. Springer-Verlag, Berlin.

ROAD, J. D. & KIRKWOOD, P. A. (1993). Distribution of monosynaptic connections from expiratory bulbospinal neurones to motoneurones of different expiratory muscles in the cat. *XXXII Congress of the International Union of Physiological Sciences* 141.39/P.

SCHMID, K., KIRKWOOD, P. A., MUNSON, J. B., SHEN, E. & SEARS, T. A. (1993). Contralateral projections of thoracic respiratory interneurones in the cat. *Journal of Physiology* **461**, 647–665.

SEARS, T. A. (1964*a*). The fibre calibre spectra of sensory and motor fibres in the intercostal nerves of the cat. *Journal of Physiology* **172**, 150–161.

SEARS, T. A. (1964*b*). Efferent discharges in alpha and fusimotor fibres of intercostal nerves of the cat. *Journal of Physiology* **175**, 386–403.

SEARS, T. A. & STAGG, D. (1976). Short-term synchronization of intercostal motoneurone activity. *Journal of Physiology* **263**, 357–381.

SHAPAVALOV, A. I. (1974). Neuronal organisation and synaptic mechanisms of supraspinal motor control in vertebrates. *Reviews of Physiology, Biochemistry and Pharmacology* **72**, 1–54.

SHINODA, Y., YAMAGUCHI, T. & FUKAMI, T. (1986). Multiple axon collaterals of single corticospinal axons in the spinal cord. *Journal of Neurophysiology* **55**, 425–448.

SWADLOW, H. A. (1982). Antidromic activation: measuring the refractory period at the site of axonal stimulation. *Experimental Neurology* **75**, 514–519.

TAYLOR, A., STEPHENS, J. A., SOMJEN, G., APPENTENG, K. & O'DONOVAN, M. J. (1977). Extracellular spike-triggered averaging for plotting synaptic projections. *Brain Research* **140**, 344–448.

VAUGHAN, C. & KIRKWOOD, P. A. (1993). Modelling of connections to inspiratory motoneurones in the anaesthetized cat. *Journal of Physiology* **473**, 17*P*.

Acknowledgements

V. Becker, M. Otto, K. Schmid and C. Vaughan each participated in one or two of the experiments. I would like to thank them for their assistance and T. A. Sears for his support and for discussions of this and related topics over many years. The work was funded by the Wellcome Trust.

Received 24 May 1994; accepted 25 August 1994.